THE ASTROPHYSICAL JOURNAL SUPPLEMENT SERIES, 107:1–17, 1996 November


# THE MORPHOLOGIES OF DISTANT GALAXIES. II. CLASSIFICATIONS FROM THE *HUBBLE SPACE TELESCOPE* MEDIUM DEEP SURVEY

ROBERTO G. ABRAHAM
Institute of Astronomy, Madingley Road, Cambridge, CB3 0HA, UK; abraham@ast.cam.ac.uk

SIDNEY VAN DEN BERGH
Dominion Astrophysical Observatory, National Research Council of Canada, 5071 West Saanich Road, Victoria, BC V8X 4M6, Canada; vdb@dao.nrc.ca

KARL GLAZEBROOK,[1] RICHARD S. ELLIS, BASILIO X. SANTIAGO, AND PETER SURMA
Institute of Astronomy, Madingley Road, Cambridge, CB3 0HA, UK; kgb@ast.cam.ac.uk, rse@ast.cam.ac.uk, santiago@ast.cam.ac.uk

AND

RICHARD E. GRIFFITHS
Department of Physics and Astronomy, Johns Hopkins University, 3400 North Charles Street, Baltimore, MD 21218; griffith@mds.pha.jhu.edu

*Received 1995 December 4; accepted 1996 April 24*

## ABSTRACT

The morphological properties of high-redshift galaxies are investigated using a sample of 507 objects ($I < 22.0$ mag) from the *Hubble Space Telescope* (*HST*) Medium Deep Survey. Independent visual morphological classifications for each galaxy are used to quantify the statistical uncertainties in the galaxy classifications. Visual classifications are found to agree well for $I < 21$ mag. Fainter than $I = 21$ mag significant disagreements are seen in the independent visual classifications of late-type systems with $T > 7$, merging systems, and peculiar galaxies. The classifications of these systems are shown to be somewhat subjective. Objective classifications based upon measurements of central concentration and asymmetry for the Medium Deep Survey sample are presented. These classifications are calibrated using measurements of structural parameters for an artificially redshifted sample of local objects. Morphologically segregated number counts using both sets of visual classifications and objective classifications support the conclusion that the observed galaxy counts agree with no-evolution predictions for the elliptical and spiral populations, as reported in Glazebrook et al. (1995a). A major conclusion is that the large overdensity of merging/peculiar/irregular galaxies relative to the predictions of no-evolution models (reported by Glazebrook et al. 1995a) is confirmed. However, the shape of the faint-end ($I > 21.0$ mag) number count relation for peculiar objects is sensitive to the large systematic uncertainties inherent in the visual classification of these objects. Despite this caveat, the frequency of objects showing clear evidence for tidal interactions (e.g., tidal tails) in the *HST* sample is at least 50% larger than it is among nearby galaxies, at the 2 $\sigma$ level. Relatively few "chain galaxies" are seen among the sample of peculiar objects, suggesting that these systems do not form a large component of the peculiar galaxy population at $I < 22$ mag.

*Subject headings:* galaxies: evolution — galaxies: fundamental parameters — galaxies: interactions — surveys

*With increasing distance, our knowledge fades, and fades rapidly. Eventually, we reach the dim boundary—the utmost limits of our telescopes. There, we measure shadows, and we search among ghostly errors of measurement for landmarks that are scarcely more substantial.*—Hubble 1936

## 1. INTRODUCTION

The Butcher-Oemler effect (Butcher & Oemler 1978) provided the first observational support (at optical wavelengths) for the view that distant galaxies are, in an evolutionary sense, younger than similar objects in our immediate neighborhood. Over the course of the last decade, photometric and spectroscopic surveys have established the view that substantial evolution has occurred in the galaxy population since $z \sim 0.5$, particularly among a population of blue star-forming objects (Broadhurst, Ellis, & Shanks 1988; Tyson 1988; Colless et al. 1990; Ellis 1990; Koo & Kron 1992; Lilly et al. 1993; Tresse et al. 1993; Cowie et al. 1994; Glazebrook et al. 1995b). The precise nature of this evolution has remained elusive, however, because these surveys have provided no direct information regarding the nature of the morphological changes that take place as galaxies age. This morphological information can be obtained only from high-resolution in situ observations of very distant galaxies. Only extremely high resolution observations with the *Hubble Space Telescope* (*HST*) can hope to provide morphological information on galaxies with redshifts $z \sim 0.5$, in which evolutionary effects are expected to become important.

Morphologically segregated number counts from a sample of 301 galaxies with $I < 22$ mag from 13 *HST* fields imaged as part of the Medium Deep Survey (MDS) have been recently reported by Glazebrook et al. (1995a). These authors find that the elliptical and spiral populations are consistent with high-normalization no-evolution models, but that the number of irregular/peculiar (possibly merging)

[1] Current address: Anglo-Australian Observatory, P.O. Box 296, Epping, NSW 2121, Australia.

galaxies is at least an order of magnitude greater than predicted. A similar conclusion has been reached by Driver, Windhorst, & Griffiths (1995) based on number counts from a single ultradeep MDS field. However, *HST* observations reported by Schade et al. (1995) of a small but spectroscopically complete sample of 32 galaxies identified in the Canada-France Redshift Survey (CFRS) suggest substantial ($\sim$1.2 mag arcsec$^{-2}$) evolution in the surface brightness of normal late-type systems at high redshift. Schade et al. find that the morphological mix at $z \sim 0.75$ is roughly similar to that seen locally, except for a population of objects outside the ordinary Hubble sequence, which Schade et al. denote as "blue nucleated galaxies" (BNGs). Schade et al. suggest that these objects comprise $\sim$35% of the blue galaxy population. The existence of another major new population of morphologically distinct objects, "chain galaxies," has also been reported by Cowie, Hu, & Songaila (1995 on the basis of *HST* observations of faint objects ($I > 23$ mag) identified in the Hawaii Deep Survey. Because of the short dynamical timescales for the destruction of gravitationally bound linear systems, Cowie et al. suggest that these objects may be protogalaxies.

It is therefore unclear whether the blue galaxy excess is due to strong evolution in the luminosity function of late-type systems, mergers/tidal interactions, or to an entirely new population of objects. Some of the ambiguity in the results from *HST* surveys may simply be due to systematic differences in the morphological classifications assigned to galaxies by different investigators. It has long been known that morphological classification is an acquired skill, but the subjectivity inherent in the galaxy classification process has only recently begun to be quantified. Naim et al. (1995) report the result from an experiment in which six experts classified independently the same 835 galaxy images (taken from the APM survey). A number of worrisome systematic effects were noted, but in the present context the most disturbing systematic is the large range (7%–23%) in the measured fraction of "peculiar" galaxies determined by experts from identical images. The Naim et al. study was done mostly using paper copies of digitized images originally taken from plate material, and observations of Virgo Cluster galaxies (van den Bergh, Pierce, & Tully 1990) show that interactive study of CCD images allows one to make morphological classifications of individual galaxies that are slightly more accurate than those that can be derived from photographic plates. However, studies of CCD images of very distant *HST* galaxies suffer from the fact that such images contain only a relatively small number of pixels. Precise classification of the images of nearby galaxies is usually based on inspection of images containing $>10^3$ pixels. *HST* images of galaxies with $I > 21$ mag typically contain at least an order of magnitude fewer pixels. While some indirect guidance can be gained by adopting classification standards that are based on artificially redshifted local archetypal galaxies, it is emphasized that *attempts to classify galaxies at large redshifts represent a considerable extrapolation from, rather than an interpolation between, nearby morphological type and class standards.* Therefore, it is important to understand which (if any) biases may be occurring in the classifications as a function of morphological type.

An important objective of current high-redshift imaging investigations is to determine whether or not the Hubble system still provides a natural framework for the classification of galaxies that are half as old as nearby extragalactic systems. As a first step in addressing this question, the present paper reports on visual and automated morphological classifications of *I*-band (F814W filter) images of a complete sample of 507 galaxies with $I < 22.0$ mag from 24 MDS fields. The specific goals of the present paper are as follows:

1. To quantify the statistical uncertainties inherent in the visual morphological classification of faint galaxy images. In this paper, *independent* sets of visual classifications are used in order to explore the systematic effects inherent in the study of distant galaxy images. It is shown that the uncertainties in visual classifications can be fairly serious even at relatively bright magnitudes ($I \gtrsim 21$) in typical deep *HST* images.
2. To argue that quantitative morphological *measurements* provide an objective route forward that will allow a reliable determination of the distribution of morphological types at $z \gtrsim 0.5$. Since it seems that *HST* may now be (or may soon be) probing redshifts and environments in which conventional classification systems may be breaking down (e.g., possible chain galaxy systems), in the future it may prove necessary to adopt formal classification systems that are not based on local archetypes.
3. To present a simple two-dimensional automated classification system that is based on the direct measurement of central concentration and asymmetry (an augmented version of the classification system presented in Abraham et al. 1994 [hereafter Paper I]). It is shown that these parameters are both physically meaningful and sufficiently robust to allow quantitative studies of galaxy morphology to be made across a large range of cosmic epoch. The techniques used to estimate central concentration and asymmetry in the present paper are completely nonparametric (unlike the case for structural parameters determined from model fits), and no a priori assumptions about the underlying forms of galaxies are required.
4. To present measurements of central concentration and asymmetry for a sample of local galaxies. These local benchmarks allow quantitative tests to be made of the hypothesis that distant galaxies differ systematically from local counterparts (and, indeed, test whether appropriate local counterparts exist).
5. To revisit the morphologically segregated number counts presented in Glazebrook et al. (1995a), using an enlarged sample of objects, independent sets of visual classifications, and objective automated classifications. The shape of the number count relation at the faint end is shown to be rather sensitive to classification uncertainties, but the basic conclusion that a substantial overdensity of tidally distorted/peculiar systems exists at high redshifts is confirmed.

## 2. MORPHOLOGICAL CLASSIFICATIONS

### 2.1. *MDS Data*

Detailed descriptions of the observational procedure used to process data for the *HST* MDS have been given elsewhere (e.g., Griffiths et al. 1994; Glazebrook et al. 1995a; Driver et al. 1995) and will only be summarized here. MDS observations are made in "parallel mode" and have an effective resolution of FWHM 0".2. Integrations were obtained in *V* (F606W) and in *I* (F814W), with typical exposure times of $\gtrsim$5000 s. At intermediate and high Galactic latitudes, the survey fields are distributed randomly over the sky. The present investigation was restricted to deep exposures (>4000 s) and fields with high galactic latitude ($|b| > 19°$). In order to isolate a sample in which morphological classifications are feasible, galaxies in the present paper have been restricted to be brighter than $I = 22.0$ mag. The majority of objects in our study have $20.0 < I < 22.0$ mag (see § 4). Recent observations by the CFRS team show that almost all galaxies in this brightness range have $0.0 < z < 1.0$, with a peak at $z \sim 0.6$ (Crampton et al. 1995). In the present work, only the $I$-band images are morphologically classified. Only a small number of MDS galaxies currently have known redshifts, but drawing flux-selected samples from Schechter-type luminosity functions at high redshift results in general in the majority of objects lying near to $L_*$.

### 2.2. *Reference Images*

#### 2.2.1. *UGC Sample and Calibration of Visual Classifications*

In order to define a reference sample for visual classification, $B$- and $V$-band CCD images of 30 local galaxies of known morphological type were artificially redshifted to $z = 0.4$–$0.8$. This reference sample was obtained as part of an ongoing project whose objective is to image a diameter-limited sample of UGC galaxies (Surma et al. 1996). Defining a reference sample with artificially redshifted objects is a crucial step in obtaining accurate visual morphological classifications. It was, for example, found that SB0 galaxies at $z \sim 0.6$ could still be recognized by their radial isophote twists and by the sharp outer edges of their lenses. Intrinsically luminous late-type "grand-design" spirals could also be recognized easily when degraded to their appearance at $z = 0.6$. However, classification of relatively compact galaxies of type Sa proved to be rather difficult and uncertain. For such objects, one has clearly reached "the utmost limits of our telescopes" at which one "searches among the ghostly errors" to which Hubble (1936) refers. For the most distant galaxies one must, following in the footsteps of Morgan (1958), use central concentration of light as the dominant classification parameter, as more subtle features are indistinguishable.[2] This idea is the inspiration behind automated classification systems based on nuclear concentration of light, such as that described in Paper I (Abraham et al. 1994) and the similar system suggested by Doi, Fukugita, & Okamura (1993).

#### 2.2.2. *Frei Sample and Calibration of Automated Classifications*

After the visual classifications were completed, a large reference sample of well-calibrated CCD images of local galaxies became available (Frei, Guhathakurta, & Gunn 1996. This sample of local galaxy images was used to calibrate the automated classifications, as described in § 2.3.2. The Frei et al. sample was particularly well suited for this purpose because the galaxies have already been preprocessed to remove contaminating foreground stars.[3] The 82 galaxies in the Frei sample imaged with the Lowell 1.1 m[4] were artificially redshifted to $z = 0.3$, 0.5, and 0.7, which span the range of redshifts expected for most objects with $I < 22$ mag. Because of the remarkable uniformity in the Frei et al. data, higher order effects (such as differential $K$-corrections in the subcomponents of the galaxy images) can be accounted for in the artificial redshifting procedure. A separate $K$-correction for each pixel in the galaxy image was determined by using a spatially resolved "color map" of the galaxy to construct a crude "spectral energy distribution (SED) map" for each point in the galaxy image. The SED map was constructed by using the color of each pixel to interpolate between a set of template SEDs (kindly supplied by A. Aragón-Salamanca) corresponding to E/S0, Sab, Sbc, and Sdm galaxies. In order to account for band-shifting effects in very blue galaxian components, a spectrum of NGC 4449 (an irregular/bursting system) was included in the sample of SED templates. A detailed description of the artificial redshifting procedure, along with multicolor images of the entire Frei sample seen over a large range of synthetic redshifts ($0.1 < z < 2$), will be presented separately (Abraham et al. 1997). Typical examples of artificially redshifted Frei galaxies are shown in Figure 1 (Plate 1).

The distribution of revised Hubble system $T$-types in the Frei sample is shown in Figure 2 of Frei et al. (1995). The objects in the Frei et al. sample are not intended to represent a fair volume-limited sample of the local universe; comparatively few very late type systems ($T > 7$), and no examples of mergers, are included. However, the objects in the Frei catalog *are* intended to be representative of "generic" early-type galaxies and late-type spirals earlier than Sdm systems. *In the present paper, the properties of the artificially redshifted Frei sample will be used to define a region of morphological parameter space occupied by "normal" galaxies with Hubble types between $T = -5$ (ellipticals) and $T = 6$ (Scd galaxies).*

### 2.3. *Classification Procedure*

The main results of the present investigation are presented in Table 1. The columns of this table provide the following information: (1) the galaxy identification number, (2) right ascension, (3) declination, (4) $I$-band magnitude, (5) central concentration, and (6) asymmetry measures defined in the next section, (7) the galaxy classification by Ellis, (8) classification by van den Bergh on the same system, (9) classification by van den Bergh on the DDO system (van den Bergh 1960a, 1960b), and (10) remarks. Ellis classifications marked by an asterisk are discussed in the notes at the end of the table. Particularly uncertain classifications are followed by a colon. Note that coordinates are accurate to within 1″–2″.

[2] We note that the idea for using central concentration to classify galaxies predates the formal specification of the Morgan system and goes back at least to Shapley (1927).

[3] Galaxies in the MDS are sufficiently small that contamination by stars on the images is not an important consideration. Removal of foreground stars prior to artificially redshifting the local images is an important step in defining a useful artificially redshifted galaxy sample for comparison with the MDS, particularly if measurements of structural parameters are to be made from the artificially redshifted images.

[4] The smaller number of images obtained with the Palomar 1.5 m telescope were not used, in order to avoid objects whose cores were saturated in the original images.

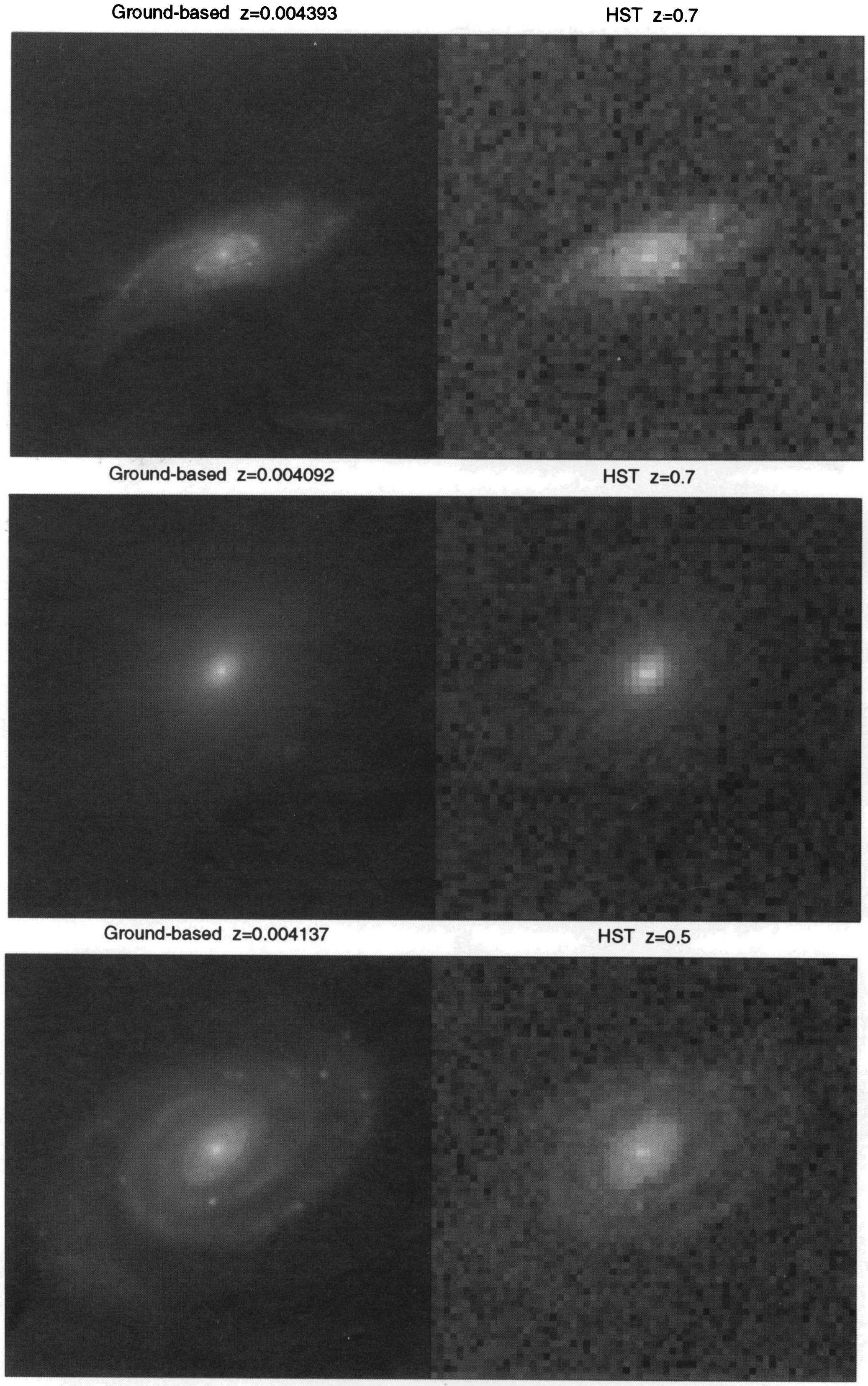


FIG. 1.—A montage showing local objects from the Frei et al. CCD sample of local galaxies (*left*), and their artificially redshifted counterparts imaged by the *HST* Wide Field Camera (*right*). Objects shown are the SAB(rs)c galaxy NGC 2715 (*top*), the E3 galaxy NGC 4365 (*middle*), and the SA(rs)bc(pec) system NGC 5364 (*bottom*). The artificially redshifted images assume 8000 s exposures through the F814W ($I$-band) filter. The sky background counts in the artificially redshifted images were calculated assuming that *HST* is pointed 15° from the north galactic cap and that the gain of the CCD controller is set to 7 electrons $ADU^{-1}$. Further details are given in the text and in Abraham et al. (1994).

ABRAHAM et al. (see 107, 3)

TABLE 1

Catalog of Morphological Classifications

| ID | RA (J2000) | Dec (J2000) | I (Mag) | C | A | RSE | VDB | DDO Class | VDB Comment |
|---|---|---|---|---|---|---|---|---|---|
| ua-0-6 | 01 02 22.4 | -27 11 25.3 | 21.00 | 0.631 | 0.159 | 7 | 0 | dE | |
| ua-0-10 | 01 02 23.4 | -27 11 21.7 | 21.60 | 0.433 | 0.018 | 3 | 4 | Sb: (edge-on) | |
| ua-0-12 | 01 02 25.3 | -27 11 23.5 | 21.01 | 0.294 | 0.169 | 1 | 0 | E1 | |
| ua-0-13 | 01 02 25.4 | -27 11 22.0 | 21.16 | ... | ... | 1 | 0 | E2 | |
| ua-0-14 | 01 02 25.7 | -27 11 21.4 | 19.45 | 0.615 | 0.149 | 2 | 1 | E6 / S0 | |
| ua-0-15 | 01 02 25.7 | -27 11 19.0 | 19.74 | ... | ... | 4 | 1 | S0: | Companion to ua-0-14. |
| ua-0-17 | 01 02 22.8 | -27 10 58.6 | 18.83 | 0.499 | 0.151 | 2 | 1 | S0 | |
| ua-0-18 | 01 02 22.9 | -27 10 54.9 | 19.77 | 0.504 | 0.196 | 3 | 4 | St | Interacting with ua-0-17. |
| ua-0-20 | 01 02 26.2 | -27 11 11.0 | 21.44 | 0.288 | 0.080 | 5 | 5 | Sc: | |
| ua-0-23 | 01 02 26.5 | -27 10 58.8 | 19.92 | 0.381 | 0.260 | 6 | 8 | St / merger | |
| ua-0-24 | 01 02 25.5 | -27 10 51.9 | 21.14 | 0.200 | 0.002 | 5 | 5 | Sc | |
| ua-0-30 | 01 02 22.7 | -27 10 31.9 | 21.52 | 0.272 | 0.028 | 5 | 5 | Sc | |
| ua-0-31 | 01 02 24.5 | -27 10 39.9 | 18.31 | 0.592 | 0.021 | 0 | 1 | E2 / S0 | |
| ua-0-34 | 01 02 24.4 | -27 10 44.3 | 21.37 | ... | ... | 7 | 7 | ? | |
| ua-0-36 | 01 02 27.3 | -27 11 4.8 | 19.99 | 0.398 | 0.074 | 3 | 4 | St | One-armed spiral. |
| ua-0-38 | 01 02 26.8 | -27 11 20.7 | 21.14 | 0.217 | 0.109 | 8 | 6 | Ir | |
| ua-0-40 | 01 02 26.5 | -27 11 37.7 | 21.81 | 0.281 | 0.111 | 4 | 4 | S pec | Has companions. |
| ua-0-46 | 01 02 27.1 | -27 11 45.1 | 21.30 | 0.242 | 0.045 | 6 | 5 | Ir IV (edge-on) | |
| ua-0-54 | 01 02 28.7 | -27 11 35.3 | 20.25 | 0.887 | 0.295 | 3 | 4 | Sb: | |
| ua-0-56 | 01 02 28.7 | -27 12 7.3 | 20.46 | 0.479 | 0.101 | 3 | 1 | S0: (edge-on) | |
| ua-0-58 | 01 02 29.7 | -27 11 43.8 | 21.97 | 0.339 | 0.113 | -1 | 3 | Sa | |
| ua-0-59 | 01 02 29.2 | -27 12 4.0 | 21.10 | 0.430 | 0.003 | 1 | 0 | E4 | |
| ua-0-62 | 01 02 31.2 | -27 11 11.6 | 20.92 | 0.466 | 0.064 | 2 | 3 | S(B)a | |
| ua-0-65 | 01 02 31.6 | -27 11 19.1 | 20.81 | 0.504 | 0.069 | 0 | 0 | E0 | |
| ua-0-68 | 01 02 31.0 | -27 11 50.7 | 21.21 | 0.296 | -0.002 | 5 | 2 | S0 (edge-on) | Dwarf? |
| ua-0-71 | 01 02 31.5 | -27 11 38.1 | 21.16 | 0.227 | 0.038 | 6 | 4 | St | Companion to ua-0-72; asymmetrical envelope. |
| ua-0-72 | 01 02 31.7 | -27 11 37.6 | 20.24 | ... | ... | 5 | 5 | Sc | |
| ua-0-73 | 01 02 30.8 | -27 12 4.6 | 21.42 | 0.392 | 0.091 | 3 | 4 | St | Distorted envelope. |
| ua-0-75 | 01 02 29.1 | -27 12 20.9 | 18.97 | 0.619 | 0.180 | 3 | 3 | Sab | |
| ua-0-82 | 01 02 26.3 | -27 12 20.0 | 20.85 | 0.271 | 0.088 | 6 | 6 | Ir | |
| ua-0-83 | 01 02 27.5 | -27 12 25.6 | 21.66 | 0.206 | 0.037 | 7 | 4 | Spec | |
| ua-0-84 | 01 02 29.0 | -27 12 33.7 | 20.39 | 0.364 | 0.044 | 3 | 4 | Sbc I: | |
| ua-0-94 | 01 02 27.1 | -27 13 4.4 | 21.98 | 0.324 | 0.175 | 4 | 4 | Sb pec | Partly resolved? Distorted envelope. |
| ubi1-1 | 01 10 2.7 | -02 27 52.1 | 20.10 | 0.343 | 0.387 | 7 | 7 | Pec or St? | Fuzzy nucleus and distant outer "arm". |
| ubi1-2 | 01 10 0.6 | -02 27 46.6 | 20.64 | 0.335 | 0.008 | 5 | 5 | Sc? | Classification based on small nucleus |
| ubi1-3 | 01 10 3.4 | -02 28 25.4 | 20.81 | 0.189 | 0.167 | 5 | 7 | Pec or Sd | |
| ubi1-5 | 01 10 0.5 | -02 28 11.2 | 21.94 | 0.282 | 0.067 | 5 | 4 | S | |
| ubi1-6 | 01 10 0.0 | -02 28 19.6 | 19.31 | 0.154 | 0.263 | 5 | 5 | Sc II: | |
| ubi1-7 | 01 10 1.8 | -02 28 36.0 | 20.97 | 0.284 | 0.085 | 4 | 6 | S/Ir | |
| ubi1-8 | 01 10 0.6 | -02 28 28.5 | 21.66 | 0.426 | 0.001 | -1 | 7 | S | Distant face-on Sc. |
| ubi1-9 | 01 10 2.2 | -02 28 44.0 | 20.83 | 0.484 | 0.003 | 0 | 0 | E0 | |
| ubi1-10 | 01 10 1.0 | -02 28 44.9 | 20.64 | 0.505 | 0.038 | 0 | 0 | E0 | |
| ubi1-11 | 01 10 1.0 | -02 28 18.1 | 21.54 | 0.356 | 0.066 | 3 | 4 | S | |
| ubi1-18 | 01 09 59.9 | -02 28 15.1 | 21.60 | ... | ... | -1 | 7 | ? | |
| ubi1-24 | 01 09 58.2 | -02 28 5.0 | 20.29 | 0.324 | 0.061 | 5 | 4 | S (edge-on) | |
| ubi1-27 | 01 09 57.4 | -02 28 6.3 | 20.18 | 0.265 | 0.052 | 5 | 7 | Pec | |
| ubi1-28 | 01 09 58.1 | -02 27 40.0 | 20.12 | 0.330 | 0.104 | 3 | 5 | SB IV: | |
| ubi1-29 | 01 09 58.5 | -02 27 23.9 | 19.67 | 0.299 | 0.114 | 3 | 4 | Sbpec | |
| ubi1-30 | 01 09 58.3 | -02 27 27.5 | 21.59 | 0.481 | 0.007 | 9 | -2 | star? | Companion to ubi1-29. |
| ubi1-31 | 01 09 58.2 | -02 27 18.8 | 20.24 | ... | ... | 8* | 6 | Ir | |
| ubi1-32 | 01 09 57.3 | -02 27 34.9 | 18.92 | 0.353 | 0.273 | 2 | 0 | E1 | |
| ubi1-35 | 01 09 55.7 | -02 27 14.3 | 20.97 | 0.282 | 0.071 | 3 | 3 | SB IV | |
| ubi1-43 | 01 09 56.9 | -02 27 32.0 | 21.97 | 0.364 | 0.019 | -1 | 7 | ? | Small, fuzzy. |
| ubi1-44 | 01 09 57.6 | -02 27 2.9 | 21.60 | 0.250 | 0.116 | 4 | 7 | Spec? | |
| ubi1-45 | 01 09 57.1 | -02 26 57.0 | 21.37 | 0.244 | 0.007 | 7 | 7 | ? | |
| ubi1-48 | 01 09 60.0 | -02 27 4.8 | 20.47 | 0.468 | 0.097 | 2 | -1 | E0 (or star) | |
| ubi1-49 | 01 09 57.7 | -02 26 23.1 | 21.86 | 0.293 | 0.021 | 3 | 3 | Sb: | |
| ubi1-50 | 01 09 58.9 | -02 26 23.9 | 19.57 | 0.625 | 0.032 | 0 | -1 | E0 or star | |
| ubi1-51 | 01 09 58.5 | -02 26 18.8 | 21.16 | 0.278 | 0.144 | 7 | 5 | Sc? | |
| ubi1-55 | 01 09 58.9 | -02 25 56.7 | 20.45 | 0.230 | 0.056 | 7 | 5 | Sct: | One-armed. |
| ubi1-56 | 01 10 1.0 | -02 26 13.4 | 20.43 | 0.388 | 0.106 | 3 | 5 | S(B)cpec | One-armed spiral with semi-stellar nucleus. |
| ubi1-58 | 01 09 59.6 | -02 26 57.8 | 21.94 | 0.167 | 0.052 | 7 | 6 | Ir V: | |
| ubi1-61 | 01 10 0.5 | -02 26 49.7 | 21.89 | 0.160 | 0.001 | 7 | ... | V | |
| ubi1-62 | 01 09 58.7 | -02 26 25.2 | 20.69 | 0.253 | 0.001 | -1 | 7 | ? | Small, fuzzy. |
| ubi1-63 | 01 10 1.6 | -02 26 40.0 | 21.64 | 0.286 | 0.020 | 4 | 4 | S? | |
| ubi1-64 | 01 10 1.0 | -02 26 29.7 | 20.89 | ... | ... | 9* | 5 | Sc | |
| ubi1-65 | 01 09 59.5 | -02 26 16.7 | 21.54 | 0.472 | 0.023 | 3 | 4 | Sb | |
| ubi1-67 | 01 10 2.3 | -02 26 16.8 | 20.74 | 0.238 | 0.075 | 4 | 7 | pec | |
| ubi1-68 | 01 10 1.2 | -02 26 5.7 | 21.60 | 0.264 | 0.084 | 7 | 7 | ? | |
| ubi1-69 | 01 10 1.0 | -02 26 30.1 | 20.95 | 0.264 | 0.087 | 3 | 5 | Sc? | |
| ucs0-1 | 02 56 25.5 | -33 22 55.6 | 21.11 | ... | ... | 8* | 6 | Ir: | |

TABLE 1—*Continued*

| ID | RA (J2000) | Dec (J2000) | $I$ (Mag) | $C$ | $A$ | RSE | VDB | DDO Class | VDB Comment |
|---|---|---|---|---|---|---|---|---|---|
| ucs0-18 | 02 56 23.8 | -33 23 45.2 | 21.67 | 0.372 | 0.036 | 4 | 4 | Sb | |
| ucs0-49 | 02 56 22.1 | -33 22 24.7 | 20.36 | 0.290 | 0.067 | 3 | 4 | SB: (or S0) | No arms visible. |
| ucs0-90 | 02 56 22.0 | -33 22 3.5 | 20.27 | 0.329 | 0.096 | 5 | 5 | Sc | |
| ucs0-91 | 02 56 21.9 | -33 22 1.0 | 21.15 | 0.326 | 0.090 | 8 | 6 | Ir + star? | Companion to ucs0-90. |
| ucs0-92 | 02 56 21.4 | -33 21 49.1 | 19.58 | 0.467 | 0.129 | 5 | 4 | Sb t? | |
| ucs0-94 | 02 56 22.9 | -33 21 57.9 | 21.62 | 0.444 | 0.039 | 4 | 1 | E7 / S0 | |
| ucs0-97 | 02 56 21.1 | -33 21 36.8 | 21.11 | 0.308 | 0.056 | 3 | 4 | Sb: | |
| ucs0-101 | 02 56 21.0 | -33 21 29.6 | 21.69 | 0.305 | 0.060 | 3 | 4 | Sb t? | Has companions. |
| ucs0-104 | 02 56 23.2 | -33 21 40.9 | 19.75 | 0.279 | 0.044 | 7 | 7 | Pec? | Disk with bright rim. |
| ucs0-105 | 02 56 24.4 | -33 21 44.3 | 21.87 | ··· | ··· | 7 | 4 | S (edge-on) | |
| ucs0-106 | 02 56 23.9 | -33 21 27.4 | 19.10 | 0.331 | 0.406 | 7 | 8 | t! | Tidally disrupted by ucs0-107. |
| ucs0-107 | 02 56 23.8 | -33 21 30.5 | 20.18 | 0.535 | 0.086 | 0 | 0 | E2 | Companion to ucs0-106. |
| ucs0-110 | 02 56 23.8 | -33 21 13.2 | 21.25 | 0.228 | 0.051 | 5 | 5 | Sc | |
| ucs0-111 | 02 56 25.2 | -33 21 21.6 | 17.52 | 0.661 | 0.025 | 2 | 0 | E5 | |
| ucs0-113 | 02 56 20.6 | -33 21 19.2 | 17.53 | 0.593 | 0.028 | 0 | 0 | E1 | |
| ucs0-117 | 02 56 20.5 | -33 21 24.9 | 20.87 | 0.139 | 0.173 | 7 | 6 | Ir IV - V: | |
| ueh0-1 | 00 53 27.7 | 12 33 35.5 | 19.34 | 0.455 | 0.024 | 1 | -1 | E0 (or star) | |
| ueh0-2 | 00 53 24.4 | 12 33 50.4 | 20.58 | 0.289 | 0.099 | 3 | 4 | S pec | Very diffuse. |
| ueh0-4 | 00 53 27.2 | 12 33 11.9 | 20.95 | 0.384 | 0.093 | 3 | 4 | S | |
| ueh0-10 | 00 53 26.1 | 12 32 42.4 | 20.16 | ··· | ··· | 0* | 4 | S | |
| ueh0-26 | 00 53 25.9 | 12 32 42.0 | 20.71 | ··· | ··· | 9 | 9 | defect (or Ir) | |
| ueh0-27 | 00 53 23.0 | 12 33 32.1 | 20.75 | 0.549 | 0.022 | 2 | 2 | SB0: | Radial isophote rotation. |
| ueh0-28 | 00 53 23.1 | 12 33 53.9 | 20.94 | 0.462 | 0.093 | 3 | 4 | St? | Asymmetrical. |
| ueh0-29 | 00 53 21.8 | 12 33 7.5 | 20.71 | 0.491 | 0.082 | 2 | 3 | Sa pec | Slightly asymmetrical. |
| ueh0-30 | 00 53 21.7 | 12 33 23.7 | 20.71 | 0.391 | 0.129 | 3 | 8 | St + S | Merger. |
| ueh0-33 | 00 53 20.7 | 12 33 7.0 | 21.26 | 0.330 | 0.069 | 5 | 5 | Sc: | No arms visible, located in group. |
| ueh0-34 | 00 53 21.2 | 12 33 50.2 | 21.61 | 0.428 | 0.002 | 0 | 3 | Sa: | |
| ueh0-35 | 00 53 20.5 | 12 33 20.2 | 21.37 | 0.250 | 0.147 | 5 | 6 | Ir: | Possibly contains off-center HII region. |
| ueh0-36 | 00 53 19.8 | 12 33 11.7 | 21.35 | 0.480 | 0.033 | 0 | 4 | S: | |
| ueh0-42 | 00 53 20.3 | 12 34 31.3 | 21.25 | 0.218 | 0.082 | 5 | 8 | merger | |
| ueh0-43 | 00 53 23.7 | 12 34 17.1 | 21.57 | 0.300 | 0.051 | 4 | 5 | Sc | |
| ueh0-46 | 00 53 23.3 | 12 34 33.7 | 21.29 | 0.270 | 0.055 | 8 | 4 | Sb (edge-on) | In a small group. |
| ueh0-49 | 00 53 23.6 | 12 34 45.4 | 20.75 | 0.328 | 0.059 | 5 | 5 | Sc | One-armed spiral? |
| ueh0-50 | 00 53 20.8 | 12 35 11.3 | 21.61 | 0.204 | 0.091 | 5 | 5 | Sm (edge-on) | |
| ueh0-51 | 00 53 22.4 | 12 35 5.4 | 21.91 | 0.368 | 0.001 | -1 | 4 | S | |
| ueh0-53 | 00 53 22.5 | 12 35 13.2 | 21.87 | 0.238 | 0.016 | 7 | 5 | Sc: | |
| ueh0-54 | 00 53 21.5 | 12 34 29.8 | 21.96 | ··· | ··· | 7 | 4 | Sb: | |
| ueh0-55 | 00 53 21.2 | 12 35 17.9 | 21.81 | 0.314 | 0.178 | 7 | 4 | S | |
| uem0-1 | 03 05 4.8 | -00 11 37.4 | 21.73 | 0.224 | 0.107 | 5 | 6 | Ir or Pec | Companion to uem0-2. |
| uem0-2 | 03 05 5.0 | -00 11 42.4 | 19.64 | 0.325 | 0.066 | 5 | 5 | SBc I | |
| uem0-4 | 03 05 7.0 | -00 12 1.1 | 21.44 | 0.534 | 0.022 | 3 | 3 | Sab | |
| uem0-9 | 03 05 6.2 | -00 12 14.9 | 21.67 | 0.438 | 0.020 | 3 | 3 | Sa | |
| uem0-25 | 03 05 2.0 | -00 11 53.3 | 20.11 | 0.378 | 0.049 | 3 | 3 | Sab | Has close companion, no tidal features. |
| uem0-26 | 03 05 2.0 | -00 11 47.0 | 21.43 | 0.316 | 0.198 | 8 | ··· | S / Ir | In a small group. |
| uem0-27 | 03 05 2.0 | -00 11 50.1 | 20.89 | 0.309 | 0.055 | 4 | 4 | S | Companion to uem0-26. |
| uem0-29 | 03 05 1.8 | -00 11 44.2 | 21.26 | 0.327 | 0.101 | 8 | 0 | Epec | Star or companion superposed. |
| uem0-31 | 03 05 1.0 | -00 11 43.3 | 20.50 | 0.292 | 0.318 | 6 | 6 | Ir or Pec | |
| uem0-33 | 03 05 0.6 | -00 11 54.0 | 20.59 | 0.566 | 0.052 | 1 | 0 | E3 | |
| uem0-38 | 03 05 0.3 | -00 11 25.3 | 21.70 | 0.228 | 0.206 | 5* | 8 | St+S | |
| uem0-41 | 03 05 0.9 | -00 10 53.7 | 21.69 | 0.242 | 0.059 | 3 | 4 | Sb | |
| uem0-42 | 03 05 0.7 | -00 11 3.9 | 21.98 | 0.416 | 0.058 | 2 | 0 | E1 | |
| uem0-43 | 03 04 59.2 | -00 11 46.6 | 19.12 | 0.437 | 0.025 | 5 | 5 | Sc I | |
| uem0-45 | 03 04 59.1 | -00 11 31.4 | 21.82 | 0.388 | 0.116 | 8* | 2 | E4 | |
| uem0-46 | 03 04 58.1 | -00 11 35.5 | 20.33 | ··· | ··· | 8 | 8 | Sa:t + E | Tidal tails and debris. |
| uem0-49 | 03 05 2.1 | -00 11 38.3 | 21.75 | 0.368 | 0.021 | 5 | 4 | Sb: | |
| uem0-60 | 03 05 1.3 | -00 10 40.4 | 21.51 | 0.131 | 0.091 | 5 | 6 | Ir or merger | Ring galaxy + perturber. |
| uem0-62 | 03 05 2.2 | -00 10 33.2 | 21.53 | 0.245 | 0.056 | 5 | 5 | Sb (edge-on) | |
| uem0-67 | 03 05 3.3 | -00 10 10.5 | 20.17 | 0.858 | 0.228 | 5 | 5 | Sc | Star superposed? |
| uem0-68 | 03 05 3.0 | -00 10 1.0 | 20.40 | 0.488 | -0.005 | 3 | 0 | E1 | In cluster? |
| uim0-1 | 03 55 33.5 | 09 43 1.9 | 20.40 | 0.506 | 0.049 | 2 | 0 | E2: | |
| uim0-7 | 03 55 33.1 | 09 42 32.8 | 21.56 | 0.485 | 0.037 | -1 | 7 | pec? | |
| uim0-8 | 03 55 31.8 | 09 42 45.9 | 20.14 | 0.486 | 0.025 | 2 | 2 | SB0 | |
| uim0-9 | 03 55 31.1 | 09 42 41.1 | 21.51 | 0.465 | 0.001 | -1 | 5 | Sc | Has semi-stellar nucleus. |
| uim0-10 | 03 55 31.3 | 09 42 29.0 | 21.55 | 0.190 | 0.067 | 7 | 5 | S IV | |
| uim0-11 | 03 55 31.5 | 09 42 15.1 | 21.23 | 0.232 | 0.329 | 8 | 8 | Sbt + S: | Interacting! |
| uim0-18 | 03 55 29.2 | 09 43 28.0 | 20.89 | 0.200 | 0.175 | 5 | 8 | Sc | Has S(t?) companions; probably interacting. |
| uim0-19 | 03 55 29.9 | 09 43 43.6 | 19.80 | 0.309 | 0.065 | 3 | 5 | S(B)c: | |
| uim0-25 | 03 55 29.3 | 09 44 1.1 | 20.33 | 0.505 | 0.046 | 2 | 0 | E4 | |
| uim0-26 | 03 55 27.4 | 09 43 29.7 | 21.99 | 0.256 | 0.001 | 7 | 7 | pec | |
| uim0-27 | 03 55 28.0 | 09 43 43.3 | 21.73 | 0.163 | 0.132 | 7 | ··· | SB: IV - V: | |
| uim0-28 | 03 55 28.5 | 09 43 53.8 | 21.73 | 0.499 | 0.020 | 2 | 2 | E2 | |
| uim0-29 | 03 55 28.3 | 09 43 40.1 | 20.97 | 0.216 | 0.900 | 8 | 8 | St: | Compact Hickson-like group, mergers. |

TABLE 1—*Continued*

| ID | RA (J2000) | Dec (J2000) | *I* (Mag) | *C* | *A* | RSE | VDB | DDO Class | VDB Comment |
|---|---|---|---|---|---|---|---|---|---|
| uim0-30 | 03 55 28.5 | 09 43 40.6 | 21.29 | 0.360 | 0.069 | 4 | 8 | Abc | Companion to uim0-29, in Hickson-like group. |
| uim0-33 | 03 55 30.7 | 09 44 18.6 | 21.83 | 0.205 | 0.087 | 7 | 5 | Sc | Has Sb companion. |
| uim0-34 | 03 55 31.1 | 09 44 14.1 | 21.76 | 0.220 | 0.499 | 7 | ... | St / pec | In Hickson-like compact group. |
| uim0-37 | 03 55 31.5 | 09 44 13.0 | 21.48 | 0.435 | 0.042 | 4 | 4 | Sb (t?) | |
| uim0-38 | 03 55 31.5 | 09 44 23.5 | 20.79 | 0.315 | 0.173 | 4 | 4 | Sbc t? | |
| uim0-41 | 03 55 33.0 | 09 44 44.0 | 18.62 | 0.442 | 0.135 | 3 | ... | Ab (t?) | Has St: companion. |
| uim0-42 | 03 55 32.0 | 09 44 59.4 | 21.74 | 0.306 | 0.031 | 7 | 5 | Sc | In a group. |
| uim0-43 | 03 55 34.0 | 09 44 41.4 | 20.59 | 0.537 | 0.059 | 4 | 3 | Sab | |
| uim0-44 | 03 55 32.3 | 09 43 52.3 | 21.98 | 0.259 | 0.047 | -1 | 4 | S: | |
| uim0-49 | 03 55 33.5 | 09 44 19.3 | 21.60 | 0.299 | 0.001 | -1 | 0 | E1: | Has Sb companion. |
| uj70-9 | 19 40 56.2 | -69 16 17.3 | 21.46 | 0.356 | 0.066 | 6 | 7 | Pec | |
| uj70-11 | 19 40 56.0 | -69 16 24.3 | 20.94 | 0.381 | 0.084 | 5 | 4 | Sb (edge-on) | |
| uj70-14 | 19 40 49.2 | -69 16 38.4 | 19.57 | ... | ... | 9 | 9 | Defect | |
| uj70-24 | 19 40 43.5 | -69 17 0.2 | 21.96 | 0.344 | 0.042 | 5 | 7 | Pec | |
| uj70-25 | 19 40 39.4 | -69 16 7.5 | 21.01 | 0.358 | 0.029 | 2 | | Pec | Small core plus large smooth envelope. |
| uj70-39 | 19 40 33.8 | -69 17 13.7 | 20.21 | ... | ... | 3 | 7 | Pec | Smooth disk with compact nucleus. |
| uj70-40 | 19 40 33.0 | -69 17 10.8 | 20.64 | 0.281 | 0.070 | 5 | 5 | S IV | Companion to uj70-39. |
| uj70-54 | 19 40 38.7 | -69 15 30.8 | 19.97 | 0.427 | 0.062 | 3 | | Pec | |
| uj70-57 | 19 40 37.2 | -69 15 32.8 | 20.68 | 0.281 | 0.052 | 3 | 0 | cD? | |
| uj70-60 | 19 40 36.1 | -69 15 28.7 | 20.63 | 0.229 | 0.291 | 5 | 6 | Ir : IV (edge-on) | |
| uj70-61 | 19 40 32.5 | -69 15 25.2 | 21.96 | 0.456 | 0.036 | -1 | 0 | E:2 | |
| uj70-63 | 19 40 39.3 | -69 15 14.0 | 21.94 | 0.363 | 0.163 | 0 | 0 | E0 | |
| uj70-64 | 19 40 38.3 | -69 15 14.7 | 21.78 | 0.541 | 0.087 | 0 | 0 | E1 | |
| uj70-71 | 19 40 38.4 | -69 14 51.9 | 20.19 | 0.541 | 0.070 | 0 | 0 | E1 | |
| uj70-74 | 19 40 28.5 | -69 15 2.6 | 15.31 | ... | ... | -2 | -2 | Star | |
| umd4-5 | 21 51 3.1 | 29 00 16.8 | 21.03 | 0.392 | 0.106 | 3 | 4 | S pec | |
| umd4-13 | 21 51 5.9 | 29 00 32.5 | 19.42 | 0.319 | 0.083 | 5 | 5 | Sc II: | |
| umd4-19 | 21 51 4.9 | 29 01 7.5 | 20.60 | 0.400 | 0.239 | 6 | 4 | S pec | |
| umd4-38 | 21 51 8.8 | 29 00 56.8 | 21.26 | 0.420 | 0.084 | 8 | 6 | Ir | |
| umd4-39 | 21 51 9.0 | 29 00 19.4 | 21.81 | 0.347 | 0.077 | 3 | 4 | Sbt | Interacting with umd4-40. |
| umd4-40 | 21 51 9.2 | 29 00 21.0 | 21.66 | 0.394 | 0.047 | 3 | 4 | Sbt | |
| umd4-41 | 21 51 9.1 | 29 01 5.2 | 19.92 | 0.303 | 0.154 | 5 | 4 | Sbc I | |
| umd4-44 | 21 51 9.4 | 29 00 8.7 | 18.97 | 0.348 | 0.110 | 5 | 4 | Sbc: | High surface brightness. |
| umd4-59 | 21 51 9.8 | 28 59 48.4 | 20.31 | 0.410 | 0.045 | 3 | 4 | Sb | |
| umd4-62 | 21 51 9.1 | 28 59 38.5 | 20.70 | 0.347 | 0.127 | 5 | 4 | S (edge-on) | Has Ir companion. |
| umd4-65 | 21 51 8.9 | 28 59 28.2 | 20.98 | 0.364 | 0.059 | 5 | 4 | S(B:)b or St | |
| umd4-74 | 21 51 9.9 | 28 59 13.8 | 21.38 | 0.287 | 0.126 | 6 | 5 | Sc III: | |
| umd4-76 | 21 51 7.3 | 28 59 7.2 | 21.27 | ... | ... | 7* | 0 | d E3 | |
| uo50-5 | 17 55 26.1 | 18 17 52.7 | 21.95 | 0.529 | 0.302 | 7 | 7 | ? In a group | |
| uo50-6 | 17 55 26.9 | 18 17 8.4 | | ... | ... | | | | |
| uo50-7 | 17 55 26.5 | 18 17 2.9 | 18.94 | 0.903 | 0.219 | 4 | 7 | Defect? | |
| uo50-13 | 17 55 25.0 | 18 17 45.1 | 21.35 | 0.540 | -0.037 | 2 | 4 | Sb | |
| uo50-15 | 17 55 24.6 | 18 17 56.2 | 20.06 | 0.226 | 0.313 | 5 | 5 | Sc I: | |
| uo50-19 | 17 55 24.2 | 18 17 57.8 | 20.86 | 0.234 | 0.099 | 0 | 4 | Sb (edge-on) | |
| uo50-20 | 17 55 24.1 | 18 17 56.2 | 21.04 | 0.240 | 0.087 | 4 | 5 | Sc | Companion to uo50-19. |
| uo50-21 | 17 55 24.3 | 18 17 50.5 | 21.51 | 0.320 | 0.261 | 5 | 5 | Sc (t?) I | |
| uo50-24 | 17 55 24.3 | 18 17 44.8 | 21.95 | 0.240 | 0.152 | 5 | 4 | Sbt (edge-on) | |
| uo50-28 | 17 55 23.4 | 18 17 53.7 | 21.93 | 0.303 | 0.317 | 3 | 5 | Sc | |
| uo50-31 | 17 55 23.9 | 18 17 2.6 | 21.36 | 0.132 | 0.364 | 5 | 4 | S (edge-on) | |
| uo50-39 | 17 55 26.5 | 18 18 21.6 | 20.93 | ... | ... | 5 | 5 | Sc | |
| uo50-45 | 17 55 25.6 | 18 18 33.4 | 21.16 | 0.390 | 0.144 | 1 | 4 | Sb | In a group. It has semi-stellar nucleus |
| uo50-58 | 17 55 23.9 | 18 18 40.5 | 20.33 | 0.240 | 0.351 | 7 | 7 | Pec | Disk with no nucleus |
| uo50-60 | 17 55 21.8 | 18 18 33.8 | 21.59 | ... | ... | 9 | 7 | ? | |
| uo50-62 | 17 55 23.7 | 18 18 45.8 | 18.34 | 0.670 | 0.362 | 1 | 0 | E3 | I in error? |
| uo50-72 | 17 55 22.1 | 18 18 57.9 | 21.46 | ... | ... | 5 | 5 | Sc: | |
| uo50-75 | 17 55 20.8 | 18 18 59.0 | 21.47 | ... | ... | 9 | ... | ... | |
| uo50-76 | 17 55 23.9 | 18 19 12.3 | 21.67 | 0.380 | -0.068 | 6 | 7 | ? | |
| uo50-80 | 17 55 27.2 | 18 18 40.5 | 21.73 | 0.710 | 0.177 | -1 | ... | ... | Star + fuzz |
| uo50-81 | 17 55 27.0 | 18 18 54.6 | 21.75 | 0.443 | 0.015 | 1 | 0 | E3 | |
| uo50-83 | 17 55 27.1 | 18 19 1.6 | 20.98 | 0.484 | -0.087 | 0 | 3 | Sa: | |
| uo50-87 | 17 55 27.6 | 18 18 55.4 | 21.65 | 0.480 | 0.062 | 1 | 4 | Sb: | |
| uo50-88 | 17 55 28.1 | 18 18 44.6 | 20.57 | 0.311 | 0.036 | 5 | 5 | Sc pec | One bright arm |
| uo50-91 | 17 55 28.7 | 18 18 36.8 | 21.27 | 0.222 | 0.074 | 6 | 8 | Merger | |
| uo50-95 | 17 55 29.5 | 18 18 38.2 | 16.35 | ... | ... | -2 | -2 | Star | |
| uo50-96 | 17 55 28.5 | 18 19 19.9 | 19.60 | ... | ... | -2 | ... | ... | Star near galaxy |
| uo50-113 | 17 55 31.7 | 18 18 43.9 | 19.97 | ... | ... | 8 | 4 | S pec | |
| uo50-118 | 17 55 30.4 | 18 19 31.5 | 21.76 | 0.413 | 0.026 | 1 | 3 | Sa: | |
| uo50-120 | 17 55 29.7 | 18 19 32.4 | 21.32 | ... | ... | 9 | 4 | S | |
| uo50-122 | 17 55 30.5 | 18 19 39.7 | 20.52 | ... | ... | 5 | 6 | Ir IV (edge-on) | |
| uo50-123 | 17 55 29.9 | 18 19 38.8 | 20.05 | ... | ... | 9 | 9 | Defect | |
| uop0-4 | 07 50 47.2 | 14 40 16.2 | 21.54 | 0.287 | -0.072 | 7 | 4 | Sbc | |
| uop0-18 | 07 50 46.5 | 14 40 32.5 | 21.87 | 0.298 | 0.001 | 4 | 4 | Sbc (edge-on) | |

TABLE 1—*Continued*

| ID | RA (J2000) | Dec (J2000) | $I$ (Mag) | $C$ | $A$ | RSE | VDB | DDO Class | VDB Comment |
|---|---|---|---|---|---|---|---|---|---|
| uop0-22 | 07 50 44.0 | 14 40 15.7 | 21.34 | 0.257 | -0.113 | 4 | 4 | Sb | Has companions of types Sc and Sc/Ir |
| uop0-24 | 07 50 46.8 | 14 40 45.9 | 21.47 | 0.109 | 0.035 | 6 | 6 | Ir IV - V: | Might be a disrupted galaxy. |
| uop0-28 | 07 50 42.7 | 14 40 29.6 | 21.54 | ... | ... | 4 | 5 | Sc | |
| uop0-30 | 07 50 43.1 | 14 40 37.8 | 21.09 | 0.244 | 0.095 | 5 | 4 | S IV | |
| uop0-32 | 07 50 43.9 | 14 40 43.2 | 16.71 | 0.601 | 0.006 | 0 | 0 | E2 | |
| uop0-34 | 07 50 44.9 | 14 40 31.9 | 19.88 | ... | ... | 3 | 3 | Sa | |
| uop0-37 | 07 50 44.9 | 14 41 11.1 | 17.64 | 0.566 | 0.032 | 2 | 1 | E7 / S0 | |
| uop0-40 | 07 50 42.0 | 14 41 10.5 | 20.72 | ... | ... | 6* | 5 | Sbc II: | |
| uop0-41 | 07 50 47.5 | 14 40 55.9 | 21.22 | ... | ... | 5 | 5 | Sc (edge-on) | Has compact nucleus. |
| uop0-44 | 07 50 47.1 | 14 41 18.7 | 21.75 | 0.356 | -0.011 | -1 | 3 | Sab: | |
| uop0-46 | 07 50 47.1 | 14 41 38.0 | 21.32 | 0.439 | -0.109 | -1 | 0 | E0 (or star) | |
| uop0-54 | 07 50 50.3 | 14 41 13.0 | 21.14 | 0.264 | -0.012 | 5 | 5 | Sbc | One-armed barred spiral has compact nucleus. |
| uop0-57 | 07 50 51.3 | 14 41 20.1 | 20.69 | 0.372 | -0.014 | 3 | 3 | Sa | Has bright nucleus. |
| usa0-6 | 17 12 21.5 | 33 35 36.0 | 21.18 | 0.453 | 0.130 | 3 | 4 | Sb + Sc | Interacting? |
| usa0-14 | 17 12 21.4 | 33 35 56.3 | 19.21 | 0.332 | 0.163 | 3 | 5 | Sc pec | Has three arms. |
| usa0-16 | 17 12 20.1 | 33 35 33.1 | 21.27 | 0.265 | 0.131 | 5 | 5 | Sc I: | |
| usa0-19 | 17 12 20.8 | 33 35 59.1 | 21.30 | 0.538 | 0.315 | 6 | 4 | S(B)bct + pec | |
| usa0-28 | 17 12 19.9 | 33 36 6.1 | 21.43 | 0.466 | 0.033 | 3 | 4 | Sb pec | One-armed spiral. |
| usa0-37 | 17 12 21.3 | 33 36 14.5 | 21.43 | ... | ... | 7 | 9 | defect? | Near edge of image. |
| usa0-39 | 17 12 20.9 | 33 36 18.9 | 21.61 | 0.420 | 0.054 | 3 | 4 | Sbt + S | |
| usa0-57 | 17 12 25.9 | 33 36 36.1 | 21.99 | 0.469 | 0.067 | 6 | 4 | S: | |
| usa0-66 | 17 12 22.1 | 33 37 17.8 | 21.84 | 0.241 | 0.087 | 6 | 4 | S IV: | |
| usa0-69 | 17 12 24.8 | 33 37 3.9 | 20.00 | 0.209 | 0.909 | 3 | 5 | Sbct | In a compact group. |
| usa0-78 | 17 12 25.2 | 33 35 47.3 | 19.03 | 0.671 | 0.121 | 3 | 2 | S0 / SB0 | |
| usa0-82 | 17 12 27.1 | 33 35 57.6 | 21.12 | 0.554 | 0.087 | 0 | 1 | E2 / Sa | |
| usa0-84 | 17 12 29.4 | 33 36 35.6 | 19.41 | ... | ... | 3 | 3 | S(B:)a | Companion to usa0-85. |
| usa0-85 | 17 12 29.5 | 33 36 33.0 | 20.86 | 0.299 | 0.376 | 5 | 8 | Sct or Sc pec | Low surface; one armed spiral. |
| usa0-87 | 17 12 27.2 | 33 35 48.6 | 20.58 | ... | ... | 7 | 5 | Sc pec? | Has semi-stellar nucleus. |
| usa0-89 | 17 12 29.6 | 33 36 25.0 | 20.88 | 0.243 | 0.107 | 5 | 5 | Sc III - IV | |
| usa0-93 | 17 12 27.5 | 33 35 30.2 | 20.95 | 0.654 | 0.111 | 0 | 0 | E3 | In compact group. |
| usa0-98 | 17 12 30.3 | 33 36 7.3 | 21.35 | 0.344 | 0.091 | 4 | 4 | S | |
| usa0-99 | 17 12 28.0 | 33 35 29.4 | 21.32 | 0.408 | 0.102 | 4 | 3 | Sab pec | Asymmetrical. |
| usa0-102 | 17 12 31.1 | 33 36 16.6 | 21.98 | 0.466 | 0.030 | -1 | -1 | E0 (or star) | |
| usa0-106 | 17 12 28.7 | 33 35 19.5 | 20.49 | 0.270 | 0.138 | 7 | 8 | merger? | Contains two nuclei. |
| usa0-108 | 17 12 30.0 | 33 35 41.0 | 21.64 | 0.308 | 0.296 | 7 | 6 | Ir | Might also be St. |
| ut20-2 | 16 01 19.3 | 05 22 58.0 | 20.72 | 0.306 | 0.039 | 7 | 4 | S | Uniform sharp-edged disk; extended. |
| ut20-3 | 16 01 19.2 | 05 23 4.3 | 21.38 | 0.291 | 0.070 | 5 | 5 | Sc | |
| ut20-4 | 16 01 19.1 | 05 23 18.0 | 20.67 | 0.298 | 0.062 | 5 | 5 | S(B) IV or Ir IV | |
| ut20-7 | 16 01 18.7 | 05 23 39.0 | 21.54 | 0.232 | 0.099 | 7 | 7 | ? | |
| ut20-9 | 16 01 19.6 | 05 23 45.1 | 21.74 | 0.222 | 0.026 | 7 | 4 | S? | Large low surface brightness object |
| ut20-15 | 16 01 21.8 | 05 23 52.0 | 18.67 | 0.587 | 0.035 | 2 | 0 | E0 (or star) | |
| ut20-16 | 16 01 21.7 | 05 23 48.8 | 19.89 | 0.558 | 0.046 | 2 | 2 | S0 (edge-on) | Companion to ut20-15. |
| ut20-17 | 16 01 22.6 | 05 23 26.8 | 21.69 | 0.300 | 0.194 | 4 | 5 | Sctpec or Sct | Distorted one-arm spiral galaxy. |
| ut20-19 | 16 01 21.3 | 05 24 21.6 | 21.36 | 0.246 | 0.749 | 9 | 7 | ... | Probably ring galaxy + perturber. |
| ut20-31 | 16 01 19.1 | 05 24 7.1 | 21.67 | 0.239 | 0.151 | -1 | 2 | SBa: | |
| ut20-32 | 16 01 22.8 | 05 23 9.6 | 21.29 | 0.284 | 0.056 | 4 | 4 | Sb: | Has Sab companion. |
| ut20-35 | 16 01 23.2 | 05 23 2.6 | 21.01 | 0.324 | 0.102 | 7 | 7 | Ir | Companion to ut20-36. |
| ut20-36 | 16 01 23.3 | 05 23 0.3 | 20.91 | 0.380 | 0.107 | 8 | 6 | Ir? | |
| ut20-39 | 16 01 23.1 | 05 22 46.3 | 20.47 | 0.518 | 0.027 | 4 | 3 | Sab | |
| ut20-40 | 16 01 23.0 | 05 22 48.7 | 20.68 | 0.488 | 0.076 | 8 | 0 | E1 (or star) | Companion to ut20-39. |
| ut20-43 | 16 01 21.3 | 05 22 9.1 | 21.00 | 0.518 | 0.036 | 4 | 4 | Sb | |
| ut20-48 | 16 01 22.6 | 05 22 20.7 | 19.56 | 0.237 | 0.107 | 5 | 5 | Sc I | |
| ut20-52 | 16 01 24.9 | 05 22 12.4 | 21.24 | 0.512 | 0.104 | 0 | -1 | E0 (or star) | |
| ut20-79 | 16 01 19.2 | 05 22 27.2 | 21.79 | 0.256 | 0.137 | 4 | 5 | Sc | Has semi-stellar nucleus; bright companion. |
| ut20-80 | 16 01 19.2 | 05 22 13.6 | 21.63 | 0.575 | 0.018 | 0 | -1 | E0 or star | |
| ut20-81 | 16 01 18.4 | 05 22 39.7 | 21.64 | 0.477 | 0.083 | 4 | 4 | Sb | |
| ut20-87 | 16 01 18.4 | 05 21 38.4 | 21.79 | 0.575 | 0.069 | -1 | 4 | Sb | |
| ut20-88 | 16 01 17.1 | 05 21 44.7 | 21.81 | 0.168 | 0.038 | 7 | ... | V: | |
| ut21-4 | 16 01 14.0 | 05 35 45.1 | 21.59 | 0.479 | 0.030 | 1 | 0 | E3 | |
| ut21-5 | 16 01 16.5 | 05 35 13.3 | 17.18 | 0.910 | 0.346 | -2 | -2 | Star | |
| ut21-6 | 16 01 15.0 | 05 35 13.4 | 21.94 | 0.169 | 0.014 | 7 | 4 | S V: | |
| ut21-7 | 16 01 13.0 | 05 35 26.6 | 21.98 | 0.411 | 0.285 | 4 | 4 | Sb | |
| ut21-9 | 16 01 12.0 | 05 35 24.9 | 21.32 | 0.289 | 0.038 | 5 | 4 | S IV | |
| ut21-12 | 16 01 14.9 | 05 34 51.8 | 21.35 | 0.367 | 0.075 | 5 | 5 | Sc | |
| ut21-14 | 16 01 14.4 | 05 34 51.1 | 21.49 | 0.159 | 0.073 | 7 | 6 | S / Ir V | |
| ut21-19 | 16 01 14.6 | 05 34 35.1 | 21.25 | 0.353 | 0.316 | 3 | 4 | Sb: | |
| ut21-20 | 16 01 12.2 | 05 34 55.7 | 21.96 | 0.272 | 0.033 | 5 | 4 | Sb (edge-on) | |
| ut21-22 | 16 01 14.1 | 05 34 30.8 | 20.55 | 0.609 | 0.114 | 0 | 0 | E2 | |
| ut21-25 | 16 01 11.3 | 05 35 32.9 | 21.21 | 0.298 | 0.091 | 3 | 5 | Sct | |
| ut21-26 | 16 01 11.1 | 05 35 34.5 | 21.77 | 0.287 | 0.099 | 7 | 6 | Ir | Interacting with ut21-25 |
| ut21-34 | 16 01 9.6 | 05 35 27.2 | 21.78 | 0.234 | 0.040 | 5 | 4 | S (edge-on) | |
| ut21-35 | 16 01 10.5 | 05 35 46.0 | 21.06 | 0.403 | 0.087 | 4 | 4 | Sp | Interacting with ut21-36 |

TABLE 1—*Continued*

| ID | RA (J2000) | Dec (J2000) | *I* (Mag) | *C* | *A* | RSE | VDB | DDO Class | VDB Comment |
|---|---|---|---|---|---|---|---|---|---|
| ut21-36 | 16 01 10.3 | 05 35 45.4 | 20.62 | ... | ... | 3 | 4 | Sbt | |
| ut21-38 | 16 01 10.4 | 05 36 5.3 | | 0.319 | 0.161 | | | | |
| ut21-40 | 16 01 8.9 | 05 35 46.2 | 20.09 | 0.517 | 0.015 | 3 | 1 | E7 / S0 (edge-on) | |
| ut21-41 | 16 01 8.9 | 05 35 53.6 | 21.38 | 0.470 | 0.016 | 1 | 0 | E2 | |
| ut21-42 | 16 01 8.5 | 05 36 7.6 | 20.44 | 0.618 | 0.013 | 3 | 0 | E0 | |
| ut21-45 | 16 01 8.3 | 05 36 13.9 | 21.39 | 0.389 | 0.263 | 5 | 4 | Sb | |
| ut21-46 | 16 01 8.2 | 05 36 12.7 | 21.52 | ... | ... | 5 | 5 | Sct | Off-center nucleus; companion:ut21-45. |
| ut21-49 | 16 01 11.6 | 05 36 27.1 | 21.75 | 0.333 | 0.129 | 3 | 4 | Sb | |
| ut21-50 | 16 01 13.1 | 05 36 12.8 | 21.29 | 0.174 | 0.275 | 6 | 6 | Ir IV (edge-on) | |
| ut21-53 | 16 01 13.0 | 05 36 27.6 | 20.54 | 0.258 | 0.056 | 4 | 5 | Sd | |
| ut21-54 | 16 01 13.1 | 05 36 32.6 | 21.74 | 0.270 | 0.226 | 6 | 4 | St | Off-center nucleus; companion:ut21-53. |
| ut21-55 | 16 01 13.6 | 05 36 27.8 | 21.56 | 0.381 | 0.242 | 3 | 4 | S | |
| ut21-58 | 16 01 10.7 | 05 37 9.2 | 21.45 | 0.302 | 0.093 | 6 | 6 | Ir | |
| ut21-62 | 16 01 12.7 | 05 37 3.0 | 21.52 | 0.270 | -0.031 | 3 | 0 | E0: Large halo | |
| ut21-63 | 16 01 13.8 | 05 36 52.9 | 21.51 | 0.231 | 0.019 | 3 | 5 | Sc | |
| ut21-65 | 16 01 14.8 | 05 37 1.6 | 20.98 | 0.338 | 0.243 | 8 | 8 | Merger? Two nuclei? | |
| ut21-69 | 16 01 15.1 | 05 37 11.1 | 19.92 | 0.479 | 0.042 | 3 | 3 | Sa: | |
| ut21-73 | 16 01 11.7 | 05 37 30.9 | 21.46 | ... | ... | 9 | 9 | Defect | |
| ut21-74 | 16 01 11.9 | 05 37 31.4 | 19.48 | ... | ... | 9 | 9 | Defect | |
| uui0-20 | 11 42 1.0 | 71 38 6.5 | 21.98 | ... | ... | 4 | 4 | Sb | |
| uui0-21 | 11 42 1.3 | 71 37 52.0 | 21.48 | 0.259 | 0.134 | 7 | 6 | Ir (edge-on) | |
| uui0-23 | 11 42 5.0 | 71 37 50.8 | 21.54 | 0.379 | 0.140 | 4 | 4 | S (edge-on) | |
| uui0-29 | 11 41 55.2 | 71 37 45.4 | 20.14 | ... | ... | 9* | 3 | Sa | In compact group |
| uui0-30 | 11 41 54.5 | 71 37 43.4 | 21.87 | 0.299 | 0.172 | 3 | 4 | St | Companion to uui0-29. |
| uui0-34 | 11 41 52.6 | 71 37 42.1 | 21.28 | 0.208 | 0.102 | 4 | 4 | St | Tidally perturbed spiral or a protogalaxy? |
| uui0-37 | 11 41 59.5 | 71 38 12.3 | 21.76 | 0.279 | 0.047 | 4 | 5 | Sc: | |
| uui0-38 | 11 41 52.0 | 71 37 53.9 | 20.93 | ... | ... | -1* | 6 | Ir IV: | Partly resolved? |
| uui0-40 | 11 41 52.4 | 71 38 1.1 | 19.97 | 0.330 | 0.071 | 3 | 7 | ? | Dwarf? |
| uui0-41 | 11 41 50.1 | 71 37 57.3 | 21.22 | 0.330 | 0.172 | 5 | 4 | S IV (edge-on) | |
| uui0-42 | 11 41 47.2 | 71 38 3.0 | 21.69 | 0.154 | 0.285 | 6 | 4 | $S^+$ IV | Partly resolved. |
| uui0-43 | 11 42 4.7 | 71 38 12.6 | 20.97 | 0.511 | 0.059 | 0 | -1 | ? | Compact, asymmetrical. |
| uui0-44 | 11 42 3.5 | 71 38 31.9 | 20.13 | 0.490 | 0.275 | 0 | 0 | E0 (or star) | Superposed on faint galaxy. |
| uui0-51 | 11 42 3.1 | 71 38 47.0 | 21.70 | ... | ... | 9* | 6 | IrIV (edge-on) | |
| uui0-54 | 11 42 8.3 | 71 38 22.3 | 20.33 | 0.313 | 0.230 | 3 | 3 | Sab t | Interacting with uui0-55. |
| uui0-55 | 11 42 9.0 | 71 38 22.5 | 20.52 | 0.237 | 0.277 | 8 | 4 | Sb t | |
| uui0-57 | 11 42 7.2 | 71 38 40.9 | 19.90 | 0.376 | 0.310 | 4 | 6 | Ir III - IV (edge-on) | |
| uui0-59 | 11 42 8.0 | 71 38 32.9 | 21.77 | 0.330 | 0.090 | 7 | 4 | Sb pec | Asymmetrical. |
| uui0-62 | 11 42 7.5 | 71 38 52.0 | 21.89 | 0.295 | 0.165 | 6 | 4 | S IV: | |
| uui0-65 | 11 42 11.8 | 71 38 34.0 | 18.68 | 0.488 | 0.170 | 0 | 0 | E3 | |
| uui0-66 | 11 42 12.1 | 71 38 37.6 | 19.70 | 0.456 | 0.549 | 0 | 0 | E3t | Interacting with uui0-65. |
| uui0-68 | 11 42 15.1 | 71 38 6.0 | 21.67 | 0.397 | 0.109 | 3 | 4 | Sb | |
| uui0-69 | 11 42 15.6 | 71 38 16.2 | 18.10 | 0.640 | 0.068 | 2 | 4 | Sab t? | High surface brightness. |
| uui0-70 | 11 42 14.9 | 71 38 17.4 | 21.16 | 0.383 | 0.081 | 2 | 2 | E / Sa: | Interacting with uui0-69. |
| uui0-71 | 11 42 14.4 | 71 38 31.0 | 21.45 | 0.512 | 0.030 | 0 | 0 | E:0 | |
| uui0-72 | 11 42 10.8 | 71 39 4.4 | 18.63 | 0.702 | 0.061 | 0 | 0 | E0 (or star) | |
| uui0-75 | 11 42 16.6 | 71 38 34.1 | 20.57 | ... | ... | 5* | 8 | Spec t? | |
| ux40-3 | 15 19 40.6 | 23 52 21.7 | 19.79 | ... | ... | 2 | 2 | S0 (edge-on) | |
| ux40-5 | 15 19 40.4 | 23 52 25.6 | 21.83 | 0.583 | 0.069 | 0 | -1 | E0 or star | Near bright galaxy. |
| ux40-6 | | | 21.24 | 0.362 | 0.198 | 0 | 8 | St + ? | Probable merger. |
| ux40-7 | 15 19 38.9 | 23 53 2.1 | 18.91 | 0.436 | 0.161 | 5 | 5 | Sct + E0 | Nucleus off-center due to tides. |
| ux40-8 | 15 19 41.1 | 23 52 22.7 | 18.57 | 0.625 | 0.045 | 0 | 0 | E0/S(B)0 | |
| ux40-11 | 15 19 38.6 | 23 53 14.8 | 21.67 | 0.294 | 0.135 | 5 | 4 | S(B)b | Companion to ux40-37. |
| ux40-16 | 15 19 41.2 | 23 52 43.8 | 20.95 | ... | ... | 7 | 7 | dE3? | Companion to ux40-17. |
| ux40-17 | 15 19 41.4 | 23 52 42.0 | 19.04 | 0.302 | 0.222 | 5 | 6 | Ir III-IV (edge-on) | Dusty! |
| ux40-24 | 15 19 40.3 | 23 53 25.7 | 21.96 | 0.261 | 0.028 | 3 | 3 | Sab: III? | Rather low surface brightness. |
| ux40-26 | 15 19 41.3 | 23 53 13.1 | 21.29 | ... | ... | 7* | 5 | Sc? | |
| ux40-27 | 15 19 42.9 | 23 52 46.2 | 20.05 | 0.285 | 0.172 | 5 | 5 | SBct | Probably distorted by ux40-29. |
| ux40-29 | 15 19 43.3 | 23 52 48.4 | 20.05 | 0.281 | 0.437 | 5 | 4 | St | Interacting with ux40-2. |
| ux40-32 | 15 19 43.8 | 23 52 48.4 | 20.75 | 0.581 | 0.050 | 0 | 0 | E0 | |
| ux40-34 | 15 19 42.5 | 23 53 21.0 | 20.72 | 0.503 | 0.019 | 0 | 0 | E5 | Companion to ux40-35. |
| ux40-35 | 15 19 42.5 | 23 53 18.4 | 20.96 | ... | ... | 3 | 0 | E4 | In a group or cluster. |
| ux40-37 | 15 19 38.6 | 23 53 8.9 | 21.81 | 0.483 | 0.046 | 3 | 3 | Sa:/E3 | Companion to ux40-11. |
| ux40-48 | 15 19 44.4 | 23 52 18.8 | 21.89 | 0.217 | 0.066 | 7 | 4 | S IV: | In cluster of LSB objects. |
| ux40-51 | 15 19 42.5 | 23 51 57.1 | 21.54 | 0.466 | 0.061 | -1 | 2 | SB0? | |
| ux40-55 | 15 19 43.2 | 23 51 40.5 | 21.73 | 0.207 | 0.117 | 6 | 7 | merger or Ir | |
| ux40-68 | 15 19 42.7 | 23 51 55.8 | 21.88 | ... | ... | -1 | 7 | ? | Companion to ux40-51. |
| ux40-86 | 15 19 40.3 | 23 51 34.7 | 19.62 | 0.256 | 0.095 | 6 | 6 | Ir IV: | Companion to ux40-87. |
| ux40-87 | 15 19 40.3 | 23 51 30.7 | 20.34 | ... | ... | 2 | 3 | Sa | |
| ux40-89 | 15 19 39.8 | 23 51 49.0 | 18.94 | 0.663 | 0.020 | 2 | 2 | S0 (edge-on) | |
| ux40-93 | 15 19 41.2 | 23 51 8.5 | 21.36 | 0.374 | 0.121 | 3 | 3 | Sab | |
| ux40-94 | 15 19 38.7 | 23 51 45.8 | 18.38 | 0.719 | 0.079 | 2 | 0 | E:5 | |
| ux40-95 | 15 19 38.6 | 23 51 41.5 | 20.80 | 0.321 | 0.075 | 0 | 0 | E0 | Companion to ux40-94. |

TABLE 1—*Continued*

| ID | RA (J2000) | Dec (J2000) | *I* (Mag) | *C* | *A* | RSE | VDB | DDO Class | VDB Comment |
|---|---|---|---|---|---|---|---|---|---|
| ux40-98 | 15 19 38.2 | 23 51 31.9 | 20.62 | 0.295 | 0.094 | 5 | 4 | S (edge-on) | |
| ux40-102 | 15 19 39.2 | 23 51 6.6 | 21.54 | 0.464 | 0.014 | 1 | 0 | E3 | In a group. |
| ux40-103 | 15 19 38.9 | 23 51 7.7 | 21.62 | 0.193 | 0.818 | 8 | 5 | Sc | Companion to ux40-102. |
| ux40-106 | 15 19 37.1 | 23 51 21.4 | 19.82 | ... | ... | 5* | 2 | S0 (edge-on) | |
| ux40-108 | 15 19 38.0 | 23 50 51.7 | 17.53 | 0.643 | 0.044 | 0 | 0 | E1 | |
| ux40-111 | 15 19 39.8 | 23 51 57.4 | 21.32 | 0.377 | 0.046 | 2 | 3 | Sa | In chain of galaxies. |
| ux40-113 | 15 19 39.8 | 23 51 55.3 | 21.25 | 0.453 | 0.037 | 3 | 2 | E/Sa | Companion to ux40-111. |
| ux40-114 | 15 19 40.5 | 23 51 27.0 | 21.86 | 0.729 | 0.015 | -1 | -2 | star | |
| ux41-2 | 15 19 55.6 | 23 45 45.3 | 21.98 | 0.318 | 0.207 | 7 | 4 | S pec | |
| ux41-4 | 15 19 56.4 | 23 45 42.5 | 21.91 | 0.271 | 0.038 | 3 | 5 | Sc | |
| ux41-10 | 15 19 57.2 | 23 45 31.2 | 21.44 | 0.286 | -0.040 | 4 | 3 | S / S0 | |
| ux41-19 | 15 19 59.9 | 23 45 34.1 | 21.57 | 0.324 | 0.150 | 6 | 7 | Star + galaxy? | |
| ux41-23 | 15 20 0.1 | 23 45 25.9 | 21.69 | 0.234 | 0.044 | 6 | 6 | Ir: (edge-on) | |
| ux41-24 | 15 20 0.2 | 23 45 18.2 | 21.56 | 0.475 | -0.010 | -2 | -1 | Star? | |
| ux41-26 | 15 19 59.6 | 23 44 55.9 | 20.67 | 0.501 | 0.187 | 4 | 3 | Sa: (edge-on) | |
| ux41-27 | 15 19 59.9 | 23 45 2.2 | 21.03 | 0.338 | 0.272 | 3 | 4 | St: + E0 | |
| ux41-30 | 15 19 57.7 | 23 44 35.6 | 20.87 | 0.295 | 0.245 | 6 | 7 | Pec | |
| ux41-32 | 15 19 55.2 | 23 44 40.1 | 21.22 | 0.426 | 0.049 | 1 | 0 | E4 | |
| ux41-33 | 15 19 55.1 | 23 44 35.6 | 21.48 | 0.280 | 0.044 | 5 | 4 | S | Companion to ux41-32 |
| ux41-38 | 15 19 58.1 | 23 44 14.9 | 20.23 | 0.555 | 0.003 | 2 | 0 | E:4 | |
| ux41-41 | 15 19 57.9 | 23 44 3.8 | 18.66 | 0.219 | 0.519 | 6 | 4 | S pec | Possible merger |
| ux41-49 | 15 19 56.2 | 23 43 40.9 | 19.82 | 0.196 | 0.425 | 8 | 6 | Ir | Partly resolved |
| ux41-50 | 15 19 53.6 | 23 44 34.3 | 21.52 | 0.202 | 0.026 | 7 | 6 | Ir | |
| ux41-53 | 15 19 53.0 | 23 44 10.5 | 21.09 | 0.306 | 0.019 | 7 | 4 | St: | |
| ux41-58 | 15 19 52.3 | 23 44 16.9 | 21.25 | 0.340 | 0.017 | 3 | 4 | Sbc | |
| ux41-59 | 15 19 51.7 | 23 43 55.3 | | ... | ... | | | | |
| ux41-60 | 15 19 51.5 | 23 43 58.6 | 21.47 | 0.236 | 0.288 | 6 | 6 | Ir | Companion to ux41-59 |
| ux41-61 | 15 19 51.5 | 23 43 55.7 | 20.76 | ... | ... | .. | 4 | St: | In a group |
| ux41-66 | 15 19 51.9 | 23 44 31.6 | 21.97 | 0.353 | 0.020 | -2 | -1 | E1 / Star | |
| ux41-69 | 15 19 51.0 | 23 44 19.4 | 21.57 | 0.322 | 0.107 | 3 | 2 | E6 / Sa | |
| ux41-73 | 15 19 51.1 | 23 44 54.3 | 21.59 | 0.199 | 0.076 | 6 | 6 | S / Ir (edge-on) | |
| ux41-77 | 15 19 50.8 | 23 45 0.7 | | ... | ... | | | | |
| ux41-81 | 15 19 49.2 | 23 44 37.9 | 20.99 | ... | ... | 3 | 5 | Sd (edge-on) | |
| uy00-3 | 14 16 17.7 | 11 32 51.4 | 21.39 | 0.272 | 0.146 | 7 | 4 | St? IV | |
| uy00-4 | 14 16 17.8 | 11 32 55.5 | 21.47 | ... | ... | 5 | 4 | St IV | Interacting with uy00-3 |
| uy00-6 | 14 16 17.9 | 11 32 42.4 | 21.68 | 0.310 | 0.236 | 7 | 5 | Sc pec | Asymmetrical. |
| uy00-9 | 14 16 18.2 | 11 33 18.0 | 19.90 | 0.351 | 0.216 | 3 | 4 | S pec | Asymmetrical. |
| uy00-10 | 14 16 18.2 | 11 33 29.1 | 18.37 | 0.614 | 0.048 | 2 | 3 | Sa pec | Asymmetrical. |
| uy00-21 | 14 16 20.0 | 11 33 49.2 | 21.68 | 0.270 | 0.026 | 4 | 5 | Sc | |
| uy00-23 | 14 16 20.4 | 11 33 50.4 | 20.68 | 0.563 | 0.019 | 4 | 3 | Sa | |
| uy00-27 | 14 16 20.9 | 11 32 38.9 | 21.64 | 0.244 | 0.112 | 7 | 6 | Ir IV (edge-on) | |
| uy00-28 | 14 16 18.2 | 11 32 24.7 | 20.42 | 0.414 | 0.049 | 3 | 2 | S0 | |
| uy00-29 | 14 16 19.3 | 11 32 27.7 | 20.96 | 0.446 | 0.031 | 4 | 3 | Sa | |
| uy00-30 | 14 16 18.3 | 11 32 19.9 | 20.87 | 0.279 | 0.028 | 6 | 4 | S IV | Companion to uy00-28. |
| uy00-35 | 14 16 18.9 | 11 32 4.2 | 19.52 | 0.445 | 0.010 | 3 | 4 | S(B)b pec | |
| uy00-36 | 14 16 19.5 | 11 31 52.3 | 21.38 | 0.213 | 0.079 | 7 | 6 | Ir | |
| uy00-40 | 14 16 22.4 | 11 31 55.1 | 21.93 | 0.211 | 0.074 | 6 | 7 | Ir / pec | |
| uy00-42 | 14 16 21.9 | 11 31 40.5 | 19.89 | 0.503 | 0.108 | 3 | 2 | S0 (edge-on) | |
| uy00-43 | 14 16 19.0 | 11 31 25.1 | 21.39 | ... | ... | 9 | 7 | ? | |
| uy00-45 | 14 16 17.6 | 11 31 56.3 | 20.66 | 0.378 | 0.061 | 6 | 6 | Ir IV (edge-on) | |
| uy00-52 | 14 16 16.4 | 11 31 57.8 | 21.26 | 0.306 | 0.210 | 7 | 6 | S / Ir IV | |
| uy00-53 | 14 16 16.3 | 11 31 55.9 | 21.25 | ... | ... | 7 | | Ir / dS: | Companion to uy00-52. |
| uy00-54 | 14 16 16.7 | 11 31 33.7 | 21.45 | 0.165 | -0.000 | 7 | 6 | Ir V | |
| uy00-58 | 14 16 15.9 | 11 31 39.5 | 21.60 | 0.328 | 0.021 | 7 | 4 | Sb: | |
| uy00-59 | 14 16 15.5 | 11 32 4.7 | 20.04 | 0.491 | 0.072 | 2 | 2 | S0 | |
| uy00-61 | 14 16 15.1 | 11 32 19.6 | 20.77 | 0.257 | -0.003 | 7 | 6 | Ir | |
| uy00-64 | 14 16 15.7 | 11 31 16.2 | 21.50 | 0.415 | 0.044 | 6 | 6 | Ir | |
| uy00-66 | 14 16 15.1 | 11 31 46.3 | 21.52 | 0.560 | 0.000 | -1 | 7 | ? | |
| uy00-67 | 14 16 14.8 | 11 31 55.5 | | 0.480 | 0.053 | | | | |
| uy00-69 | 14 16 15.0 | 11 31 21.1 | 21.85 | 0.281 | 0.033 | 4 | 4 | S | |
| uy00-70 | 14 16 14.3 | 11 31 55.2 | 21.29 | 0.375 | 0.021 | -1 | 3 | Sa: | |
| uy00-72 | 14 16 13.4 | 11 32 6.1 | 19.70 | 0.415 | 0.055 | 2 | 1 | E3 / S0 | |
| uy00-73 | 14 16 13.6 | 11 31 55.7 | 21.63 | 0.426 | 0.018 | -1 | 3 | Sa: | |
| uy00-74 | 14 16 13.8 | 11 31 36.0 | 20.77 | 0.421 | 0.082 | 4 | 4 | Sb | |
| uy00-75 | 14 16 13.9 | 11 31 24.8 | 20.50 | 0.249 | -0.012 | 5 | 2 | dS0: | Large envelope |
| uy00-76 | 14 16 13.6 | 11 31 12.7 | | 0.294 | 0.223 | | | | |
| uy00-77 | 14 16 13.6 | 11 31 14.7 | | ... | ... | | | | |
| uy40-5 | 14 34 45.7 | 25 08 38.3 | 21.62 | 0.258 | 0.092 | 8 | 8 | merger or Ir | |
| uy40-8 | 14 34 47.5 | 25 08 36.6 | 21.68 | 0.388 | 0.061 | 0 | 0 | E1 | |
| uy40-9 | 14 34 47.1 | 25 08 41.6 | 20.10 | 0.652 | 0.074 | 2 | 3 | Sa (edge-on) | Companion to uy40-10. |
| uy40-10 | 14 34 47.2 | 25 08 39.9 | 20.13 | 0.318 | 0.827 | 8 | 8 | E: + | E:t |
| uy40-34 | 14 34 46.5 | 25 08 58.8 | 21.26 | ... | ... | -2 | -2 | star | |

TABLE 1—*Continued*

| ID | RA (J2000) | Dec (J2000) | I (Mag) | C | A | RSE | VDB | DDO Class | VDB Comment |
|---|---|---|---|---|---|---|---|---|---|
| uy40-38 | 14 34 48.7 | 25 08 10.6 | 21.26 | 0.410 | 0.028 | 7 | 1 | Epec or S0pec | Slightly distorted. |
| uy40-41 | 14 34 49.6 | 25 08 25.9 | 20.21 | ... | ... | 5* | 4 | Sb/S0 (edge-on) | |
| uy40-47 | 14 34 51.2 | 25 08 56.3 | 20.41 | 0.301 | 0.071 | 3 | 4 | Sb | |
| uy40-49 | 14 34 50.2 | 25 08 0.2 | 21.63 | 0.354 | 0.032 | 7 | 0 | E:6 | |
| uy40-50 | 14 34 50.4 | 25 08 5.2 | 21.46 | 0.258 | 0.043 | 5 | 5 | Sct | One-armed spiral, compantion to uy40-54. |
| uy40-51 | 14 34 51.0 | 25 08 31.4 | 20.99 | 0.293 | 0.033 | 5 | 5 | Sbc | |
| uy40-54 | 14 34 50.6 | 25 07 60.0 | 21.70 | 0.195 | 0.049 | 7 | 5 | Scd | Semi-stellar nucleus. Companion to uy4-50. |
| uy40-55 | 14 34 50.6 | 25 07 50.1 | 21.51 | 0.223 | 0.110 | 5 | 5 | S IV: | |
| uy40-59 | 14 34 51.8 | 25 07 53.4 | 21.73 | 0.455 | 0.037 | 4* | 0 | E:1 | |
| uy40-60 | 14 34 52.2 | 25 08 6.1 | 21.98 | ... | ... | 8* | ... | Sbc+Star | |
| uy40-64 | 14 34 53.6 | 25 08 17.6 | 21.89 | 0.368 | 0.076 | 1 | 0 | E1 | Star? |
| uy40-67 | 14 34 50.4 | 25 08 13.5 | 21.75 | 0.252 | 0.001 | 7 | 4 | Sbc | No direct evidence for interactions with |
| uy40-82 | 14 34 50.9 | 25 07 27.9 | 21.39 | 0.464 | 0.020 | 0 | 0 | E0 | |
| uy40-83 | 14 34 50.4 | 25 07 29.3 | 21.68 | 0.358 | 0.161 | -1 | 6 | Ir | Compact, partly resolved. |
| uy40-84 | 14 34 51.8 | 25 07 14.3 | 17.72 | ... | ... | 5 | 4 | Sbc III: | Partly resolved. |
| uy41-1 | 14 35 33.4 | 25 17 46.9 | 21.16 | 0.274 | 0.166 | 5 | 5 | Sc t: | Probably distorted by companion. |
| uy41-7 | 14 35 32.1 | 25 17 38.0 | 20.30 | 0.603 | 0.090 | 2 | 3 | Sa | |
| uy41-9 | 14 35 31.6 | 25 17 49.4 | 19.92 | 0.358 | 0.136 | 5 | 4 | S pec (edge-on) | Contains bright knots. |
| uy41-10 | 14 35 31.7 | 25 17 58.6 | 20.55 | 0.591 | 0.052 | 0 | 0 | E3 | |
| uy41-11 | 14 35 31.6 | 25 17 56.1 | 21.87 | 0.591 | 0.043 | 7 | 2 | S0: | Companion to uy41-10. |
| uy41-12 | 14 35 30.9 | 25 17 15.6 | 18.75 | 0.505 | 0.253 | 8 | 8 | Merger | |
| uy41-18 | 14 35 29.7 | 25 17 37.6 | 21.83 | ... | ... | 8 | 4 | S ? t | Companion to uy41-17. |
| uy41-24 | 14 35 28.7 | 25 17 2.5 | 21.35 | 0.374 | 0.171 | 4 | 0 | E6 | |
| uy41-25 | 14 35 28.9 | 25 17 53.2 | 20.72 | 0.507 | 0.184 | 0 | 2 | S0? pec | Slightly asymmetrical. |
| uy41-30 | 14 35 28.1 | 25 17 14.6 | 21.78 | ... | ... | 0 | 2 | S0? | |
| uy41-38 | 14 35 32.2 | 25 18 27.9 | 21.41 | 0.205 | 0.030 | 3 | 5 | Sc | |
| uy41-58 | 14 35 29.3 | 25 19 19.0 | 20.05 | 0.324 | 0.258 | 8 | 8 | Merger | three nuclei. |
| uy41-67 | 14 35 36.5 | 25 19 3.5 | 19.09 | 0.592 | 0.098 | 2 | 2 | S0 | |
| uy41-79 | 14 35 38.4 | 25 19 6.3 | 19.94 | 0.709 | 0.087 | 0 | 0 | E1 | |
| uzk0-4 | 12 11 12.9 | 39 27 36.4 | 21.15 | ... | ... | 3 | 3 | Sab | |
| uzk0-8 | 12 11 14.1 | 39 27 23.4 | 20.29 | ... | ... | 5 | 5 | Sc I | |
| uzk0-9 | 12 11 13.9 | 39 27 49.4 | 21.67 | ... | ... | 9 | ... | ... | Part of tidal tail of uzk0-10. |
| uzk0-10 | 12 11 14.0 | 39 27 52.8 | 19.84 | 0.432 | 0.203 | 6 | 4 | St! | Has tidal tails. |
| uzk0-12 | 12 11 14.8 | 39 27 42.2 | 21.69 | 0.338 | -0.100 | -1 | 4 | S | |
| uzk0-14 | 12 11 16.2 | 39 27 20.0 | 21.40 | 0.422 | -0.037 | 3 | 4 | Sb: | |
| uzk0-15 | 12 11 15.0 | 39 28 23.7 | 20.53 | ... | ... | -2 | | E0 + debris | |
| uzk0-18 | 12 11 16.1 | 39 28 13.9 | 21.66 | 0.288 | 0.082 | 7 | 7 | ? | Crossed by defect? |
| uzk0-20 | 12 11 16.9 | 39 27 52.8 | 21.41 | 0.501 | 0.033 | 4 | 4 | S: | |
| uzk0-36 | 12 11 14.9 | 39 26 53.6 | 19.98 | 0.502 | 0.053 | 3 | 3 | SBab | |
| uzk0-37 | 12 11 15.6 | 39 26 54.9 | 21.17 | 0.361 | 0.053 | 4 | 3 | Sa | |
| uzk0-52 | 12 11 19.0 | 39 26 27.7 | 20.53 | 0.401 | 0.075 | 8 | 4 | S: pec | |
| uzk0-75 | 12 11 11.9 | 39 25 59.3 | 21.96 | 0.308 | 0.030 | 3 | 4 | Sb | |
| uzk0-80 | 12 11 10.7 | 39 26 23.1 | 20.52 | 0.533 | 0.044 | 3 | 0 | E:2 | Shows isophote rotation. |
| uzk0-81 | 12 11 10.4 | 39 26 34.2 | 20.52 | 0.417 | 0.049 | 1 | 4 | S | |
| uzk0-82 | 12 11 10.2 | 39 26 47.8 | 21.33 | 0.396 | 0.051 | -1 | 4 | S: | |
| uzk0-84 | 12 11 9.5 | 39 26 34.0 | 21.92 | 0.230 | 0.302 | 7 | 7 | Ir or merger | |
| uzk0-90 | 12 11 8.9 | 39 25 47.4 | 21.41 | 0.524 | 0.191 | -1 | 4 | Sb: | |
| uzp0-4 | 11 50 28.2 | 28 48 56.0 | 21.76 | 0.398 | -0.015 | 2 | 0 | E:2 | Companion to uzp0-5 |
| uzp0-5 | 11 50 28.5 | 28 48 58.0 | 18.91 | 0.344 | 0.214 | 3 | 4 | Sbt | |
| uzp0-6 | 11 50 28.6 | 28 48 59.7 | 18.88 | ... | ... | 5 | 4 | SBb t | |
| uzp0-8 | 11 50 27.4 | 28 49 23.1 | 21.67 | 0.290 | 0.034 | 3 | 4 | Sb | |
| uzp0-15 | 11 50 27.3 | 28 49 40.7 | 21.74 | ... | ... | 5 | 5 | Sbct | Nucleus off- center; in a group. |
| uzp0-24 | 11 50 28.4 | 28 49 50.6 | 21.31 | ... | ... | 3 | 4 | Sb: | |
| uzp0-27 | 11 50 30.7 | 28 49 10.0 | 19.47 | ... | ... | 8 | 8 | Merger? | Two nuclei? |
| uzp0-28 | 11 50 29.5 | 28 49 40.1 | 20.60 | 0.285 | 0.067 | 5 | 5 | Sc IV: | |
| uzp0-29 | 11 50 29.8 | 28 49 52.7 | 21.55 | 0.251 | 0.053 | 6 | 5 | Sc | In a group |
| uzp0-32 | 11 50 31.9 | 28 49 2.9 | 20.96 | 0.234 | -0.045 | 7 | 4 | S IV | |
| uzp0-36 | 11 50 31.5 | 28 49 29.4 | | 0.306 | 0.122 | | | | |
| uzp0-42 | 11 50 32.0 | 28 49 33.8 | 20.94 | 0.234 | 0.011 | 5 | 5 | Sc II | |
| uzp0-56 | 11 50 32.8 | 28 48 25.9 | 20.55 | 0.430 | 0.176 | 3 | 7 | Pec | |
| uzp0-60 | 11 50 32.0 | 28 48 14.4 | 19.40 | 0.671 | 0.106 | 2 | 0 | E5 | |
| uzp0-67 | 11 50 33.6 | 28 48 7.6 | 18.64 | 0.554 | 0.024 | 3 | 2 | S(B)a pec | Has two outer tidal arms or jets. |
| uzp0-73 | 11 50 35.8 | 28 48 4.3 | 21.60 | 0.221 | 0.206 | 6 | 6 | Ir pec | |
| uzp0-79 | 11 50 30.2 | 28 47 37.4 | 19.54 | 0.354 | 0.466 | 4 | 7 | Pec | Central disk embedded in S0-like envelope. |
| uzp0-80 | 11 50 29.6 | 28 47 45.2 | 21.17 | 0.352 | 0.393 | 6 | 6 | Ir | |
| uzp0-84 | 11 50 29.7 | 28 47 23.1 | 21.08 | 0.301 | 0.103 | 5 | 6 | Ir? | Smooth, no nucleus. |
| uzp0-89 | 11 50 28.6 | 28 47 39.8 | 21.55 | 0.228 | 0.213 | 6 | 4 | S IV | |
| uzp0-100 | 11 50 27.6 | 28 47 30.4 | 21.93 | 0.275 | -0.017 | 7 | 4 | Sb | |
| uzp0-102 | 11 50 26.1 | 28 48 5.0 | 19.61 | 0.488 | 0.079 | 3 | 4 | Sb | |
| uzp0-107 | 11 50 27.8 | 28 47 10.8 | 20.98 | 0.453 | 0.051 | 4 | 4 | Sb? | |
| uzp0-109 | 11 50 26.0 | 28 47 55.5 | 21.05 | 0.495 | 0.133 | 2 | 3 | Sa: | |
| uzp0-110 | 11 50 26.4 | 28 47 44.0 | 21.37 | 0.238 | 0.008 | 5 | 5 | Sc: | |

TABLE 1—*Continued*

| ID | RA (J2000) | Dec (J2000) | $I$ (Mag) | $C$ | $A$ | RSE | VDB | DDO Class | VDB Comment |
|---|---|---|---|---|---|---|---|---|---|
| uzp0-111 | 11 50 27.0 | 28 47 27.4 | 20.88 | 0.367 | 0.094 | 5 | 5 | Sbc pec | Incomplete spiral arms. |
| uzp0-112 | 11 50 26.3 | 28 47 23.5 | 21.02 | 0.569 | 0.091 | 0 | -1 | E0 / star | |
| uzp0-116 | 11 50 24.9 | 28 47 49.0 | 21.89 | 0.326 | 0.064 | 6 | 6 | Ir (edge-on) | |
| uzp0-117 | 11 50 25.4 | 28 47 33.0 | 19.94 | 0.318 | 0.175 | 5 | 5 | Sc | |
| uzp0-118 | 11 50 24.5 | 28 47 59.6 | 19.08 | 0.560 | 0.067 | -1 | 7 | Pec | |

NOTES.—uem0-38: Image shows two nuclei and tidal tails. This is clearly an interacting/merging pair.
uem0-45: No obvious signs of interaction.
uy40-41: Nucleus too large for Sc classification.
uy40-53: This is not a low surface brightness spiral.
uy40-60: No direct evidence for interactions.
ux40-26: Type Sc assigned because of small nucleus and faint disk. However, no spiral arms are visible.
ux40-106: Probably S0 rather than Sc because no arms are visible.
ubil-31: No sign of tidal arms, so probably not a merger.
ubil-64: Not an image defect.
ueh0-10: Not as compact as an elliptical.
ucs0-1: This appears to be a partly resolved Ir galaxy rather than a merger remnant.
uop0-40: It has a nucleus, so it must be a spiral.
uui0-29: This is an Sa spiral.
uui0-38: This may be a partly resolved Ir galaxy.
uui0-51: Edge-on dwarf irregular. Not an image defect.
uui0-75: Merger remnant? Has two nuclei and one spiral arm.
umd4-76: Appears to be a low surface brightness dE3.

### 2.3.1. *Visual Classifications*

The classifications in columns (7) and (8) are on the following scale (which is consistent with that adopted by Glazebrook et al. 1995a): $-2$ = star, $-1$ = compact, 0 = E, 1 = E/S0, 2 = S0, 3 = Sab, 4 = S, 5 = Scdm, 6 = Ir, 7 = peculiar, 8 = merger, and 9 = defect. Each bin spans roughly three revised Hubble $T$-types. Note that the $S = 4$ classification represents a wide bin corresponding to spirals of unknown class. Classifications on the DDO system are most valuable for those objects that can be morphologically typed more finely than the bins given above, and for denoting those objects that show some signs of tidal disturbance or other peculiarity but which are not sufficiently distorted to warrant classification as type 7 or 8.

### 2.3.2. *Automated Classifications*

Independently from the visual classifications, automated measurements were made of central concentration ($C$) and rotational asymmetry ($A$). As described in Abraham et al. (1994), $C$ was measured from the second-order moments of the images. These moments were determined within an isophotal area enclosed by pixels 1.5 $\sigma$ above the sky level. The corresponding limiting surface brightness varied between $\mu = 24.3$–$25.1$ mag arcsec$^{-2}$ (due to variations in exposure time and intrinsic sky background level). At $I < 22$ mag, galaxies are sufficiently large that the *HST* point-spread function (PSF) does not affect appreciably measures of $C$, and hence Monte Carlo simulations were not required to calibrate the central concentration measurements. Simulations were made, however, in order to estimate the error in $C$ introduced by the different limiting isophote levels on the CCD frames. Since this error was found to be fairly small ($\sigma_C \sim 0.05$, for $\Delta\mu = 0.5$ mag arcsec$^{-2}$), raw $C$ values were used without making any correction for variations in the limiting isophote.

The asymmetry parameter $A$ was determined by rotating individual galaxy images about their centers and self-subtracting these from the original galaxy images. The parameter $A$ is defined to be half the ratio of the absolute value of the total light in the self-subtracted image to the total light in the original image (after sky subtraction). The center of rotation was determined by first smoothing the galaxy image with a Gaussian kernel of $\sigma = 1$ pixel and then choosing the location of the maximum pixel as the center. Since the absolute value of the residual light is used, noise in the images shows up as a small positive $A$ signal even in perfectly symmetrical objects. A small correction factor is therefore subtracted from the measured asymmetry value in order to account for this. This correction factor is simply the value of $A$ for a portion of sky with area equal to that enclosed by the galaxy isophote. A small amount of the false $A$ signal (due to the excess Poisson noise in the galaxy light relative to the sky noise + read noise) remains in the final estimate for this parameter for bright galaxies, but this is sufficiently small ($\sigma_A \lesssim 0.05$) that it does not significantly affect galaxy classifications.

The positions on the $C$-$A$ diagram of the artificially redshifted galaxies from the Frei et al. sample are shown in Figure 2 (Plate 2). These reference objects define an envelope on the $C$-$A$ plane, and the positions of objects on this diagram can be used to subdivide the data into two natural morphological bins: (1) $E$/S0s and (2) intermediate–to–late type-spirals. While there is some overlap between Sa and S0 systems on the $C$-$A$ diagram, there is a striking separation between the early-type systems and intermediate–to–late-type spirals. A third bin (very late type spirals/irregulars/mergers) is defined as the region the diagram to the upper left of the intermediate–to–late-type spiral bin; this is something of an extrapolation, but this extrapolation seems justified by (*a*) the a priori knowledge that these objects are not in the Frei sample, (*b*) the expectation that these systems will be relatively nonnucleated and quite asymmetric, and (*c*) the observed position of many bright MDS objects classified visually as Sdm/irregular/peculiar/mergers in this portion of the diagram (described in § 3.2).

The measurements of central concentration and asymmetry for the original and artificially redshifted Frei sample

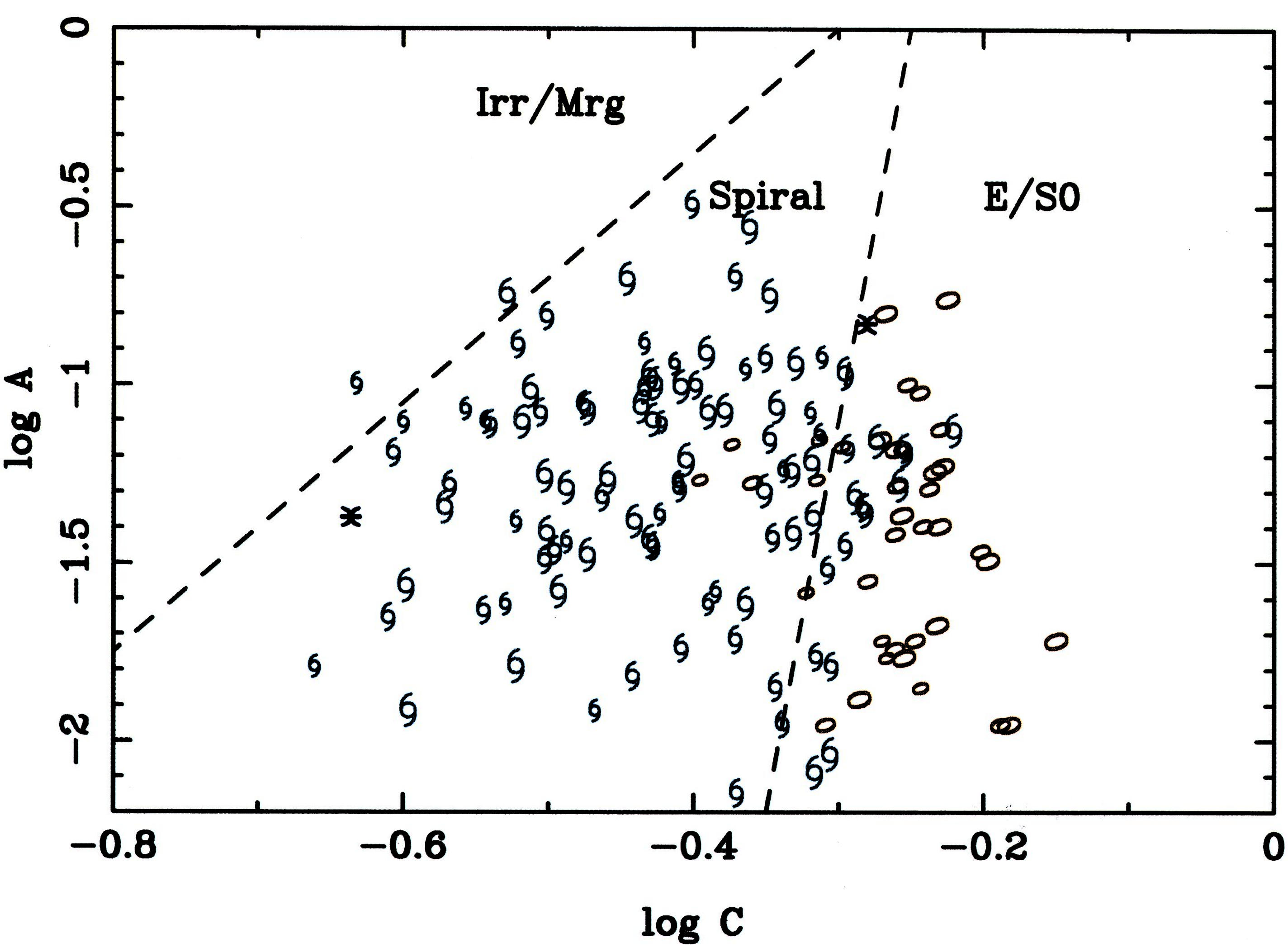


FIG. 2.—The distribution on the *C-A* plane of artificially redshifted galaxies from the Frei sample. Only objects with $I < 22$ are shown. Plot symbols denote E/S0 systems (*red ellipses*), spirals (*light blue spiral symbols*), and irregulars (*dark blue asterisks*). The sizes of the plot symbols are inversely proportional to the artificial redshifts of the galaxies (which can be one of $z = 0.3$, 0.5, or 0.7). Dashed lines delineate the three morphological bins adopted in the present work.

ABRAHAM et al. (see 107, 11)

are given in Table 2 (where the information on morphological types was obtained from the NASA Extragalactic Database compendium of information from the Third Reference Catalog of de Vaucouleurs et al. 1991). The robustness of these parameters to image degradation resulting from increased line-of-sight distance is illustrated in Figure 3. Both parameters are seen to be remarkably robust to degradation: there is a slight systematic change in $\Delta C$ (as the galaxy images become affected by sampling effects) and increased scatter at fainter magnitudes, but random measurement errors dominate the error term out to $I \gtrsim 21.5$.

TABLE 2

FREI SAMPLE CALIBRATION

| ID | RC3 Class | $T$ | $\epsilon$ | $C$ | $A$ | $I_{z=0.3}$ | $C_{z=0.3}$ | $A_{z=0.3}$ | $I_{z=0.5}$ | $C_{z=0.5}$ | $A_{z=0.5}$ | $I_{z=0.7}$ | $C_{z=0.7}$ | $A_{z=0.7}$ |
|---|---|---|---|---|---|---|---|---|---|---|---|---|---|---|
| N2683 | SA(rs)b | 3 | 0.743 | 0.514 | 0.083 | 20.95 | 0.514 | 0.048 | 22.42 | 0.425 | 0.200 | 23.40 | 0.459 | 0.057 |
| N2715 | SAB(rs)c | 5 | 0.627 | 0.335 | 0.067 | 20.25 | 0.315 | 0.038 | 21.55 | 0.285 | 0.023 | 22.48 | 0.259 | 0.001 |
| N2768 | E6: | -5 | 0.541 | 0.515 | 0.014 | 18.90 | 0.549 | 0.066 | 20.33 | 0.527 | 0.001 | 21.47 | 0.473 | 0.001 |
| N2775 | SA(r)ab | 2 | 0.178 | 0.466 | 0.001 | 18.82 | 0.556 | 0.065 | 20.16 | 0.508 | 0.066 | 21.21 | 0.460 | 0.001 |
| N2976 | SAc pec | 5 | 0.511 | 0.299 | 0.313 | 24.68 | — | — | — | — | — | — | — | — |
| N2985 | (R')SA(rs)ab | 2 | 0.178 | 0.498 | 0.001 | 19.32 | 0.558 | 0.001 | 20.70 | 0.520 | 0.045 | 21.72 | 0.479 | 0.083 |
| N3077 | I0pec | 90 | 0.158 | 0.490 | 0.103 | 24.70 | — | — | — | — | — | — | — | — |
| N3079 | SB(s)c | 5 | 0.811 | 0.444 | 0.269 | 19.75 | 0.435 | 0.276 | 21.08 | 0.397 | 0.320 | 22.04 | 0.368 | 0.130 |
| N3147 | SA(rs)bc | 4 | 0.134 | 0.440 | 0.018 | 17.96 | 0.480 | 0.060 | 19.38 | 0.451 | 0.037 | 20.47 | 0.412 | 0.026 |
| N3166 | SAB(rs)0a | 0 | 0.503 | 0.595 | 0.012 | 19.18 | 0.657 | 0.011 | 20.61 | 0.636 | 0.001 | 21.72 | 0.619 | 0.001 |
| N3184 | SAB(rs)cd | 6 | 0.179 | 0.229 | 0.012 | 20.79 | 0.253 | 0.012 | 22.12 | 0.245 | 0.022 | 23.14 | 0.218 | 0.016 |
| N3344 | (R)SAB(r)bc | 4 | 0.037 | 0.357 | 0.084 | 20.62 | 0.325 | 0.051 | 21.90 | 0.288 | 0.077 | 22.84 | 0.295 | 0.024 |
| N3351 | SB(r)b | 3 | 0.216 | 0.439 | 0.009 | 19.64 | 0.466 | 0.038 | 21.04 | 0.453 | 0.014 | 22.07 | 0.393 | 0.001 |
| N3368 | SAB(rs)ab | 2 | 0.273 | 0.555 | 0.028 | 18.98 | 0.601 | 0.074 | 20.34 | 0.556 | 0.066 | 21.43 | 0.486 | 0.072 |
| N3377 | E5-6 | -5 | 0.380 | 0.534 | 0.001 | 20.75 | 0.591 | 0.059 | 21.93 | 0.667 | 0.001 | 23.20 | 0.476 | 0.026 |
| N3379 | E1 | -5 | 0.140 | 0.541 | 0.022 | 19.24 | 0.584 | 0.057 | 20.59 | 0.570 | 0.095 | 21.73 | 0.537 | 0.019 |
| N3486 | SAB(r)c | 5 | 0.168 | 0.476 | 0.025 | 21.50 | 0.482 | 0.008 | 22.68 | 0.512 | 0.001 | 23.83 | 0.358 | 0.001 |
| N3556 | SB(s)cd | 6 | 0.665 | 0.321 | 0.159 | 20.36 | 0.307 | 0.095 | 21.76 | 0.247 | 0.064 | 22.78 | 0.233 | 0.100 |
| N3596 | SAB(rs)c | 5 | 0.118 | 0.377 | 0.050 | 20.45 | 0.362 | 0.041 | 21.82 | 0.326 | 0.001 | 22.74 | 0.321 | 0.001 |
| N3623 | SAB(rs)a | 1 | 0.703 | 0.424 | 0.036 | 19.12 | 0.445 | 0.050 | 22.14 | 0.425 | 0.019 | 21.60 | 0.378 | 0.078 |
| N3631 | SA(s)c | 5 | 0.090 | 0.346 | 0.069 | 19.77 | 0.366 | 0.086 | 21.06 | 0.344 | 0.048 | 21.97 | 0.353 | 0.001 |
| N3672 | SA(s)c | 5 | 0.569 | 0.381 | 0.108 | 19.25 | 0.371 | 0.105 | 20.59 | 0.334 | 0.087 | 21.57 | 0.300 | 0.041 |
| N3675 | SA(s)b | 3 | 0.438 | 0.419 | 0.084 | 20.32 | 0.468 | 0.114 | 21.74 | 0.390 | 0.018 | 22.71 | 0.407 | 0.024 |
| N3726 | SAB(r)c: | 5 | 0.386 | 0.255 | 0.050 | 21.09 | 0.252 | 0.027 | 22.37 | 0.218 | 0.001 | 23.41 | 0.194 | 0.001 |
| N3810 | SA(rs)c | 5 | 0.303 | 0.458 | 0.108 | 20.13 | 0.465 | 0.057 | 21.41 | 0.426 | 0.007 | 22.35 | 0.388 | 0.053 |
| N3877 | SA(s)c: | 5 | 0.763 | 0.413 | 0.119 | 20.59 | 0.393 | 0.061 | 21.97 | 0.319 | 0.034 | 22.96 | 0.316 | 0.001 |
| N3893 | SAB(rs)c: | 5 | 0.266 | 0.441 | 0.088 | 20.06 | 0.454 | 0.086 | 21.41 | 0.446 | 0.118 | 22.37 | 0.394 | 0.006 |
| N3938 | SA(s)c | 5 | 0.090 | 0.400 | 0.082 | 20.33 | 0.373 | 0.079 | 21.59 | 0.361 | 0.015 | 22.50 | 0.283 | 0.001 |
| N3953 | SB(r)bc | 4 | 0.501 | 0.397 | 0.050 | 19.34 | 0.407 | 0.083 | 20.70 | 0.389 | 0.051 | 21.70 | 0.340 | 0.012 |
| N4013 | Sb | 3 | 0.779 | 0.247 | 0.127 | 22.63 | 0.312 | 0.001 | 24.08 | — | — | — | — | — |
| N4030 | SA(s)bc | 4 | 0.225 | 0.508 | 0.028 | 18.80 | 0.532 | 0.069 | 20.18 | 0.506 | 0.035 | 21.09 | 0.469 | 0.001 |
| N4088 | SAB(rs)bc | 4 | 0.625 | 0.308 | 0.194 | 20.75 | 0.296 | 0.177 | 21.97 | 0.301 | 0.129 | 22.99 | 0.251 | 0.078 |
| N4123 | SB(r)c | 5 | 0.379 | 0.296 | 0.020 | 20.37 | 0.314 | 0.055 | 21.64 | 0.275 | 0.004 | 22.66 | 0.273 | 0.001 |
| N4125 | E6pec? | -5 | 0.392 | 0.504 | 0.001 | 18.76 | 0.586 | 0.021 | 20.16 | 0.566 | 0.019 | 21.31 | 0.541 | 0.017 |
| N4136 | SAB(r)c | 5 | 0.061 | 0.340 | 0.039 | 22.18 | 0.336 | 0.085 | 23.62 | 0.331 | 0.001 | 24.66 | 0.279 | 0.001 |
| N4144 | SAB(s)cd?sp | 6 | 0.759 | 0.384 | 0.064 | 24.16 | — | — | 25.28 | — | — | — | — | — |
| N4157 | Sbc | 5 | 0.807 | 0.430 | 0.129 | 18.84 | 0.406 | 0.122 | 20.12 | 0.399 | 0.099 | 21.02 | 0.377 | 0.043 |
| N4242 | SAB(s)dm | 8 | 0.260 | 0.236 | 0.008 | 21.99 | 0.231 | 0.042 | 23.37 | 0.236 | 0.001 | 24.33 | — | — |
| N4340 | SB(r)0+ | -1 | 0.250 | 0.472 | 0.030 | 20.90 | 0.535 | 0.001 | 22.27 | 0.561 | 0.001 | 23.48 | 0.425 | 0.001 |
| N4365 | E3 | -5 | 0.229 | 0.529 | 0.001 | 19.32 | 0.561 | 0.001 | 20.77 | 0.529 | 0.001 | 21.92 | 0.470 | 0.001 |
| N4374 | E1 | -5 | 0.022 | 0.533 | 0.001 | 18.94 | 0.588 | 0.040 | 20.40 | 0.566 | 0.001 | 21.49 | 0.554 | 0.066 |
| N4406 | S0(3)/E3 | -5 | 0.293 | 0.479 | 0.001 | 24.19 | — | — | 26.04 | — | — | — | — | — |
| N4429 | SA(r)0+ | -1 | 0.509 | 0.500 | 0.038 | 19.31 | 0.518 | 0.013 | 20.74 | 0.482 | 0.001 | 21.88 | 0.423 | 0.068 |
| N4442 | SB(s)0$^0$ | -2 | 0.578 | 0.593 | 0.006 | 21.17 | 0.708 | 0.019 | 22.10 | 0.648 | 0.011 | 23.56 | 0.775 | 0.001 |
| N4449 | IBm | 10 | 0.385 | 0.442 | 0.119 | 22.82 | 0.524 | 0.147 | 23.99 | — | — | — | — | — |
| N4450 | SA(s)ab | 2 | 0.369 | 0.462 | 0.001 | 18.09 | 0.494 | 0.009 | 19.40 | 0.458 | 0.011 | 20.51 | 0.426 | 0.001 |
| N4472 | E2/S0(2) | -5 | 0.184 | 0.530 | 0.001 | 18.61 | 0.571 | 0.004 | 19.95 | 0.548 | 0.038 | 21.10 | 0.504 | 0.067 |
| N4477 | SB(s)0:? | -3 | 0.095 | 0.516 | 0.001 | 22.11 | 0.554 | 0.043 | 20.63 | 0.525 | 0.028 | 21.80 | 0.509 | 0.006 |
| N4486 | E0-1 | -4 | 0.177 | 0.534 | 0.002 | 17.86 | 0.556 | 0.017 | 19.22 | 0.548 | 0.018 | 20.39 | 0.507 | 0.001 |
| N4487 | SAB(rs)cd | 6 | 0.362 | 0.303 | 0.024 | 21.31 | 0.300 | 0.016 | 22.73 | 0.314 | 0.001 | 23.75 | 0.244 | 0.001 |
| N4526 | SAB(s)0$^0$: | -2 | 0.646 | 0.586 | 0.080 | 21.10 | 0.596 | 0.174 | 22.50 | 0.559 | 0.100 | 23.69 | 0.417 | 0.001 |
| N4564 | E6 | -5 | 0.503 | 0.576 | 0.001 | 20.29 | 0.635 | 0.032 | 21.70 | 0.628 | 0.034 | 23.00 | 0.486 | 0.070 |
| N4593 | (R)SB(rs)b | 3 | 0.285 | 0.457 | 0.023 | 18.43 | 0.481 | 0.042 | 19.83 | 0.464 | 0.006 | 20.81 | 0.426 | 0.003 |
| N4594 | SA(s)a | 1 | 0.466 | 0.465 | 0.107 | 18.04 | 0.522 | 0.044 | 19.49 | 0.495 | 0.016 | 20.60 | 0.481 | 0.001 |
| N4621 | E5 | -5 | 0.348 | 0.533 | 0.001 | 21.43 | 0.540 | 0.159 | 22.91 | 0.573 | 0.040 | 24.03 | — | — |
| N4636 | E0-1 | -5 | 0.281 | 0.484 | 0.001 | 19.11 | 0.526 | 0.004 | 20.57 | 0.491 | 0.011 | 21.65 | 0.489 | 0.001 |
| N4710 | SA(r)0+?sp | -1 | 0.671 | 0.588 | 0.083 | 19.85 | 0.535 | 0.070 | 21.27 | 0.437 | 0.053 | 22.32 | 0.402 | 0.054 |
| N4731 | SB(s)cd | 6 | 0.626 | 0.300 | 0.089 | 20.43 | 0.303 | 0.078 | 21.88 | 0.270 | 0.052 | 22.89 | 0.254 | 0.001 |
| N4754 | SB(r)0:- | -3 | 0.442 | 0.583 | 0.004 | 19.30 | 0.628 | 0.001 | 20.74 | 0.589 | 0.075 | 21.80 | 0.571 | 0.014 |
| N4826 | (R)SA(rs)ab | 2 | 0.452 | 0.383 | 0.028 | 19.86 | 0.418 | 0.084 | 21.26 | 0.368 | 0.096 | 22.30 | 0.432 | 0.110 |
| N4861 | SB(s)m: | 9 | 0.653 | 0.243 | 0.068 | 22.89 | 0.228 | 0.001 | 24.42 | — | — | — | — | — |
| N4866 | SA(r)0+:sp | -1 | 0.749 | 0.392 | 0.001 | 20.46 | 0.410 | 0.001 | 21.85 | 0.365 | 0.001 | 23.04 | 0.388 | 0.001 |

TABLE 2—*Continued*

| ID | RC3 Class | $T$ | $\epsilon$ | $C$ | $A$ | $I_{z=0.3}$ | $C_{z=0.3}$ | $A_{z=0.3}$ | $I_{z=0.5}$ | $C_{z=0.5}$ | $A_{z=0.5}$ | $I_{z=0.7}$ | $C_{z=0.7}$ | $A_{z=0.7}$ |
|---|---|---|---|---|---|---|---|---|---|---|---|---|---|---|
| N5005 | SAB(rs)bc | 4 | 0.577 | 0.480 | 0.050 | 19.26 | 0.506 | 0.107 | 20.57 | 0.492 | 0.030 | 21.62 | 0.488 | 0.119 |
| N5204 | SA(s)m | 9 | 0.402 | 0.328 | 0.067 | 24.51 | — | — | 25.99 | — | — | — | — | — |
| N5248 | SAB(rs)bc | 4 | 0.443 | 0.381 | 0.082 | 19.49 | 0.390 | 0.098 | 20.78 | 0.373 | 0.035 | 21.78 | 0.325 | 0.036 |
| N5322 | E3-4 | -5 | 0.342 | 0.529 | 0.001 | 18.24 | 0.597 | 0.005 | 19.59 | 0.579 | 0.051 | 20.70 | 0.549 | 0.001 |
| N5334 | SB(rs)c: | 5 | 0.226 | 0.208 | 0.001 | 21.19 | 0.244 | 0.001 | 22.58 | 0.215 | 0.001 | 23.65 | 0.185 | 0.001 |
| N5364 | SA(rs)bcpec | 4 | 0.405 | 0.360 | 0.044 | 19.81 | 0.371 | 0.036 | 21.16 | 0.333 | 0.001 | 22.25 | 0.271 | 0.001 |
| N5371 | SAB(rs)bc | 4 | 0.296 | 0.333 | 0.042 | 17.87 | 0.347 | 0.054 | 19.15 | 0.314 | 0.032 | 20.21 | 0.278 | 0.001 |
| N5377 | (R)SB(s)a | 1 | 0.571 | 0.515 | 0.028 | 19.44 | 0.552 | 0.052 | 20.86 | 0.483 | 0.017 | 22.08 | 0.430 | 0.001 |
| N5585 | SAB(s)d | 7 | 0.380 | 0.358 | 0.051 | 23.46 | 0.326 | 0.001 | 24.98 | — | — | — | — | — |
| N5669 | SAB(rs)cd | 6 | 0.307 | 0.321 | 0.066 | 20.92 | 0.321 | 0.026 | 22.38 | 0.276 | 0.001 | 23.37 | 0.281 | 0.001 |
| N5701 | (R)SB(rs)0/a | 0 | 0.053 | 0.567 | 0.025 | 19.58 | 0.581 | 0.001 | 21.05 | 0.550 | 0.052 | 22.27 | 0.484 | 0.054 |
| N5746 | SAB(rs)b?sp | 3 | 0.792 | 0.488 | 0.197 | 18.66 | 0.449 | 0.177 | 20.08 | 0.449 | 0.070 | 21.15 | 0.386 | 0.114 |
| N5792 | SB(rs)b | 3 | 0.607 | 0.374 | 0.187 | 19.55 | 0.358 | 0.197 | 20.99 | 0.315 | 0.155 | 21.98 | 0.277 | 0.085 |
| N5813 | E1-2 | -5 | 0.288 | 0.484 | 0.001 | 19.56 | 0.483 | 0.001 | 21.07 | 0.438 | 0.001 | 22.25 | 0.414 | 0.001 |
| N5850 | SB(r)b | 3 | 0.301 | 0.434 | 0.001 | 18.99 | 0.467 | 0.001 | 20.45 | 0.436 | 0.001 | 21.62 | 0.422 | 0.001 |
| N5985 | SAB(r)b | 3 | 0.489 | 0.343 | 0.046 | 18.50 | 0.336 | 0.033 | 19.89 | 0.296 | 0.002 | 20.96 | 0.260 | 0.001 |
| N6015 | SA(s)cd | 6 | 0.534 | 0.391 | 0.048 | 20.94 | 0.374 | 0.100 | 22.21 | 0.312 | 0.083 | 23.21 | 0.286 | 0.078 |
| N6118 | SA(s)cd | 6 | 0.601 | 0.272 | 0.039 | 19.90 | 0.268 | 0.045 | 21.25 | 0.233 | 0.001 | 22.36 | 0.198 | 0.001 |
| N6384 | SAB(r)bc | 4 | 0.326 | 0.427 | 0.043 | 18.88 | 0.432 | 0.024 | 20.26 | 0.395 | 0.001 | 21.37 | 0.362 | 0.001 |
| N6503 | SA(s)cd | 6 | 0.653 | 0.479 | 0.074 | 24.47 | — | — | — | — | — | — | — | — |

## 3. COMPARISON OF CLASSIFICATIONS

### 3.1. *Visual versus Visual Classifications*

A comparison of the Ellis (RSE) and van den Bergh (vdB) classifications is shown in Figure 4*a*. This figure is a "Tukey box plot" (Tufte 1993) showing the distribution of classification made by the second observer as a function of the classifications made by the first observer. Individual plot symbols summarize the shape of the distribution for each classification bin. The boxes in this figure enclose the 25th and 75th percentiles for the data, while the vertical line shows the range spanned by the 10th–90th percentiles. The horizontal line indicates the median, with the gray area encompassing the 90% confidence intervals on the median. Individual circles and asterisks indicate the positions of very discrepant outliers in the data. The Spearman-Rank correlation coefficient,[5] $\rho$, for various subsets of visual classifications is given in Table 3. For the entire data set $\rho = 0.676$, improving to $\rho = 0.772$ for the subset of galaxies with $I < 21$ mag. For faint objects ($21 < I < 22$ mag), the correlation is much poorer, with $\rho = 0.576$.

TABLE 3

Spearman-Rank Correlation Coefficients

| Subset | vdB vs. RSE | $C$ vs. RSE | $C$ vs. vdB |
|---|---|---|---|
| All data .......... | 0.676 | 0.624 | 0.636 |
| $I < 21$ ............ | 0.772 | 0.662 | 0.674 |
| $21 < I < 22$...... | 0.576 | 0.552 | 0.584 |

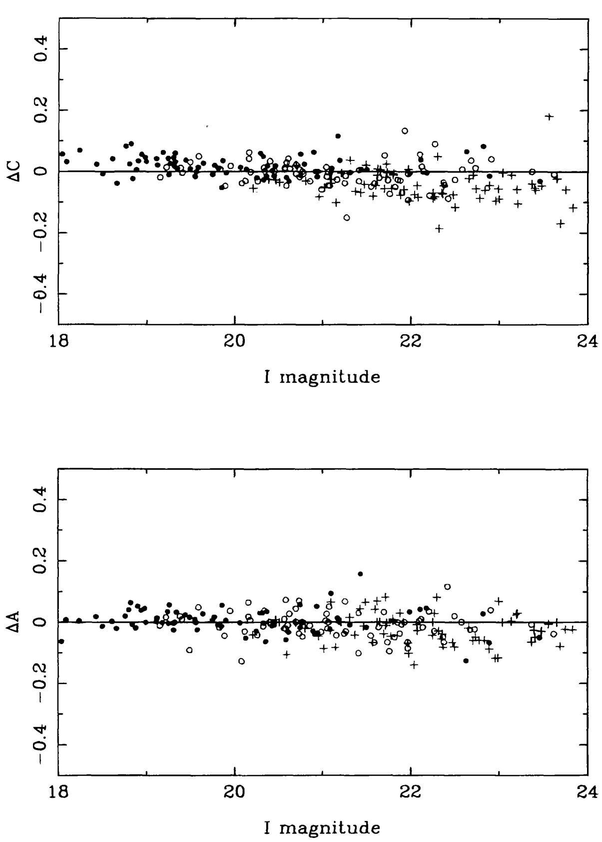


Fig. 3.—Measurement errors for $C$ (*top*) and $A$ (*bottom*), determined from the artificially redshifted Frei control sample. The uncertainties are quantified in terms of $\Delta C = C_{\mathrm{high}\,z} - C_{\mathrm{local}}$ and $\Delta A = A_{\mathrm{high}\,z} - A_{\mathrm{local}}$. The distributions are shown for $z = 0.3$ (*points*), $z = 0.5$ (*open circles*), and $z = 0.7$ (*crosses*). For $I < 22$ mag, $\sigma_C = 0.042$ and $\sigma_A = 0.043$.

Overall, the comparison of the visual classifications indicates a rather good agreement between independent classifications for early to intermediate types, especially for $I < 21$ mag. However, significant problems occur in bins 7 and 8 (the peculiar bin and the merger bins). Eliminating objects classified by RSE as 7 or 8 increases the correlation to $\rho = 0.738$. As found by Naim et al. (1995), classification into these categories is particularly subjective. For example, the large scatter in the RSE and vdB classifications for these categories is probably the result of vdB assigning galaxies to types 7 and 8 only if they showed obvious large distortions or tidal tails, whereas RSE included more subtle distortions and close pairs of galaxies in these categories. In nearby MDS objects, tidal tails have surface brightness $\mu_I \sim 24$ mag arcsec$^{-2}$, so with $(1 + z)^4$ cosmological dimming tidal debris in more distant objects has an $I$-band surface bright-

[5] The Spearman-Rank correlation coefficient is closely related to Kendall's $\tau$ statistic and is more robust than product-moment correlation coefficients in the presence of outliers. We note also that the precise value of the correlation coefficient is sensitive to the morphological binning scheme used to parameterize the visual classifications.

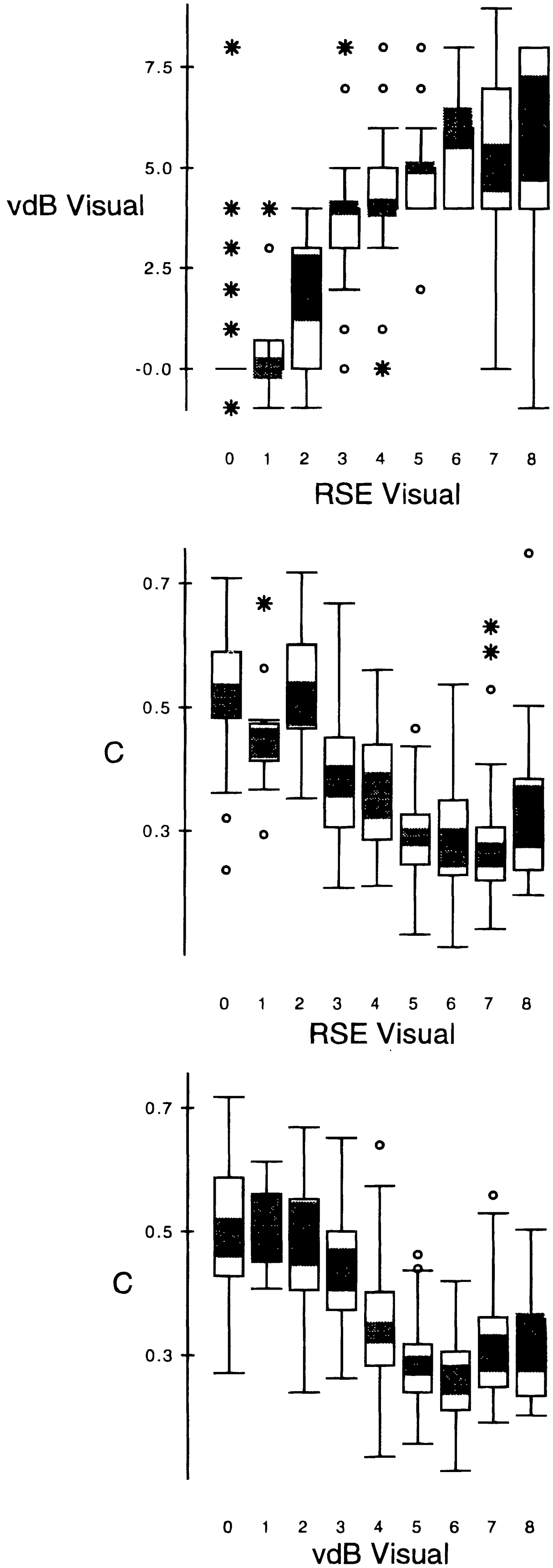


FIG. 4.—Box plots comparing the sets of morphological classifications. *Top:* Visual vs. visual classifications. Note the good agreement between classifications, except for classes 7 (peculiar) and 8 (merger). *Middle:* Central concentration vs. RSE visual classification. *Bottom:* Central concentration vs. vdB visual classification. See text for further details.

ness that is often below the detection limit in MDS images, and hence classification of mergers among faint objects is particularly difficult. It should, however, be emphasized that image size, rather than apparent magnitude, is the most important factor affecting the accuracy of the morphological classification of distant galaxies, and that evolutionary brightening in young populations within tidal debris may partly counteract the effects of cosmological dimming.

### 3.2. *Visual versus Automated Classifications*

The correlation between the vdB and RSE classifications and the central concentration parameter $C$ is shown in Figures 4*b* and 4*c*. The correlation coefficient for $C$ versus vdB classification ($\rho = 0.636$) and $C$ versus RSE classification ($\rho = 0.624$) is only slightly lower than that for visual classification ($\rho = 0.676$). This is because the galaxies in our sample are predominantly faint (57% of the sample is at $I > 21$ mag), and when spiral arms are too faint to be visible the classification of faint galaxies is based mostly on apparent bulge-to-disk ratio, which is tracked by the $C$ parameter. In fact, Table 3 suggests that for objects fainter than $I = 21$ mag *classifications based on the single parameter $C$ are as accurate as visual classifications.* For brighter objects ($I < 21$ mag) for which more morphological information is available, the correlation between the two sets of visual classifications rises quickly, while the correlation with central concentration is only slightly improved ($\rho = 0.662$ for $C$ vs. RSE, and $\rho = 0.674$ for $C$ vs. vdB). The reason for the lack of improvement at brighter magnitudes is seen in Figures 4*b* and 4*c*: classifications based on central concentration alone cannot resolve the fine distinction between various categories of early-type systems, and $C$ also does not allow intermediate-to-late-type spirals to be distinguished from very late types and irregulars. The former difficulty is fairly intractable, since the visual distinction between E and S0 objects is notoriously subtle, but the latter difficulty can be alleviated by introducing the asymmetry parameter $A$ into the classification scheme. In Figures 5 and 6 (Plates 3–4) objects are classified into the three morphological bins in the $C$-$A$ diagram described in § 2.3.2, determined from artificially redshifted local galaxies. Classificaions that incorporate the asymmetry parameter are better able to distinguish between intermediate-type spirals and very late type/irregular/merging systems. Since the three crude morphological bins advocated in the present work correspond closely to the simple elliptical, spiral, and peculiar bins arrived at independently by Glazebrook et al. (1995a) for their number count analysis, it appears that surveys based on objective measurements of the simple $C$ and $A$ parameters contain sufficient morphological informaton to form the basis for meaningful statistical studies of faint galaxy morphology.

## 4. FREQUENCY OF HUBBLE TYPES

The morphologically segregated luminosity functions of local galaxies can be determined using well-established nonparametric estimators (e.g., Efstathiou, Ellis, & Peterson 1988; Marzke et al. 1994), so the local frequency of Hubble types can be determined in an essentially model-independent manner from magnitude-limited surveys, and the results from local magnitude-limited surveys (such as the CfA1 and Shapley-Ames surveys) can be intercompared directly. Because of the large redshift range probed by the Medium Deep Survey, however, cosmological effects can

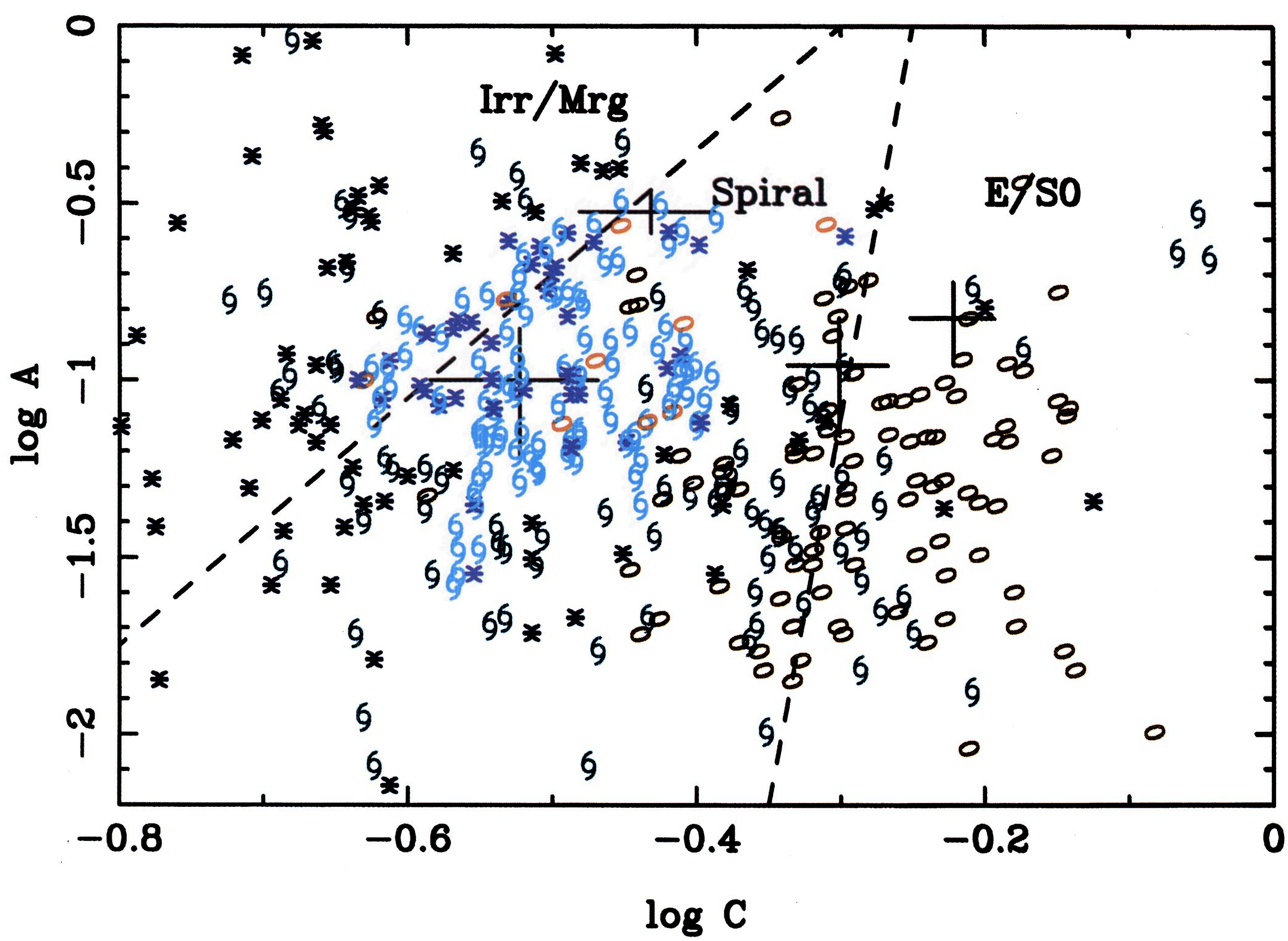


FIG. 5.—The distribution of MDS galaxies on the central concentration ($C$) vs. asymmetry ($A$) plane. Plot symbols and colors are keyed to the visual classifications of RSE. Symbols are as follows: objects classified as "compact" galaxies, ellipticals, and S0s (classes 0, 1, and 2) are shown as ellipses; objects classified as Sab, S, and Scdm (classes 3, 4, and 5) are shown using spiral symbols; objects classified as irregulars, peculiars, or mergers (classes 6, 7, and 8) are shown as asterisks. Representative error bars corresponding to different portions of the diagram are shown. The sectors of the plane delineating early, late, and irregular/peculiar/merger bins defined from the artificially redshifted local galaxy sample shown in Fig. 2 are indicated.

ABRAHAM et al. (see 107, 14)

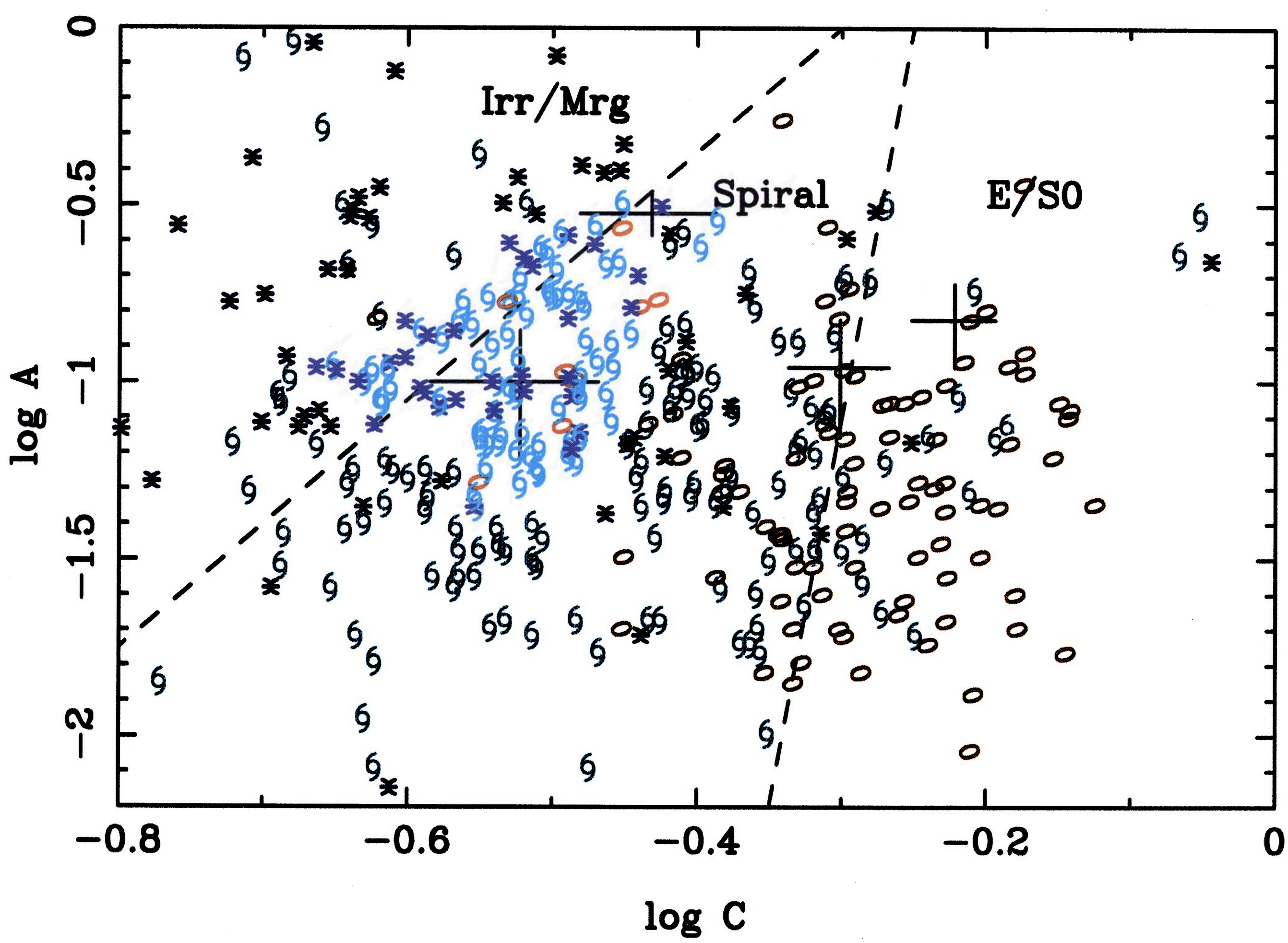


FIG. 6.—Same as Fig. 5, except with plot symbols keyed on the classifications of vdB

dominate the selection criteria for the sample.[6] In order to convert the observed fractions of the various morphological classes seen in the MDS into space densities (for comparison with local data), one must make assumptions with regard to both the form of the local luminosity function and the spectral characteristics of the sample. Following Glazebrook et al. (1995a), the present paper assumes the local luminosity functions of Loveday et al. (1992) in order to compare the observed number counts from the MDS with the predictions of no-evolution, high local normalization models.

### 4.1. *Number Counts*

Figure 7 (Plate 5) illustrates the morphologically segregated (using RSE classifications) number counts as a function of magnitude, using the format adopted in Glazebrook et al. (1995a). This figure has been updated to include the additional RSE classifications presented here. Superposed on this figure are the number counts resulting from vdB and automated classifications for the same sample of galaxies. The lines are the no-evolution predictions described in Glazebrook et al. (1995a) for $\phi_* = 0.03\ h^3\ \mathrm{Mpc}^{-3}$ (*solid*) and for $\phi_* = 0.015\ h^3\ \mathrm{Mpc}^{-3}$ (*short-dashed*) normalizations. The extra curve on the E/S0 panel shows the effect of a flat faint-end luminosity function for $\phi_* = 0.03\ h^3\ \mathrm{Mpc}^{-3}$. All three sets of classifications are in excellent agreement with the no-evolution models for $I < 21$ mag, and the large overabundance of irregular/peculiar/merging systems reported in Glazebrook et al. (1995a) is confirmed. The slope of the number count relation for spirals and irregular/peculiar/merger systems is similar. However, fainter than $I > 21$ mag, the vdB number count relation for E/S0s and irregular mergers flatten, while the corresponding RSE counts steepen. Automated counts for irregular mergers lie in between the RSE and vdB counts at faint magnitudes. As described in § 3.1, beyond $I = 21$ mag the morphological classification of very late type systems versus peculiar/merging systems is rather uncertain. Figure 7 suggests that this uncertainty can affect the detailed shape of the number count relation at the faint end, but not the fundamental conclusion that these systems are greatly in excess of predictions based on local samples.

The inherent subjectivity in defining a sample of peculiar systems is probably being exacerbated by the rather coarse binning imposed by the numerical classification system used in the present paper. The data given in column (9) of Table 1 list Hubble types on the DDO system (van den Bergh 1960a, 1960b), and it is seen that many objects have been flagged as tidally distorted (suffixed by t or t?) or peculiar (suffixed by pec or pec?) without being given numerical indices of 7 or 8. So it appears that a large part of the factor of 2 discrepancy in the number counts for peculiar/irregular/merger systems in Figure 7 results from making the distinction between, say, an Sct (class 4) and a merger (class 8), or between an S0pec (class 2) and a peculiar system (class 7).

A comparison between the frequency of the flattening values for elliptical galaxies (estimated visually) in Table 1 with the corresponding frequency distributions (normalized to E3) of elliptical galaxies in the Revised Shapely-Ames Catalog (RSA) (Sandage & Tammann 1981) and in the Second Reference Catalog (RC2) (de Vaucouleurs, de Vaucouleurs, & Corwin 1976), is shown in Figure 8. The *HST* data exhibit an excess of E0 galaxies compared to the axial ratio distribution observed among galaxies in the RSA, although the excess is not significantly different from that seen in the RC2, and hence the significance of this excess is difficult to interpret. It is seen in Figure 1 that high-redshift ellipticals can appear visually rounder than their local counterparts because of the high concentration of light in the undersampled cores of compact, concentrated objects. Tests indicate also that the automated star-galaxy separation algorithm can fail under a number of circumstances (such as when a spike of light falls on the intersection of four pixels, or when cosmic-ray clipping truncates the cores of stars), so it is possible that some contamination between stars and compact ellipticals may have occurred in Table 1. It is rather difficult to distinguish between faint compact galaxies and stars on the MDS images, and weak contamination by stars may be responsible for the fact that Driver et al. (1995) find some elliptical "galaxies" to be quite blue.

### 4.2. *The Nature of Peculiar Systems*

Because the interpretation of the number counts presented in the previous section is sensitive to assumptions made with regard to the normalization and faint-end slope of the local luminosity function, it is interesting to consider what *model-independent* statements can be made directly from the raw numbers given in Table 1. From this table, it is seen that the great majority (88%) of *HST* galaxies in the MDS sample still find a home within the Hubble classification scheme (i.e., they are not classed as peculiars or mergers using the vdB numerical scale, which will be adopted throughout this subsection, as it is the most conservative in terms of flagging objects as unusual). By contrast, 94% of the 935 nearby Shapley-Ames galaxies that were classified on the same system by van den Bergh (1960c) fit comfortably within the Hubble system. Together, "irregular" plus peculiar and merger galaxies account for 21% of the distant *HST* sample, compared to only 9% of the nearby Shapley-Ames sample, and 7% in the CfA1 + CfA2 sample. Therefore, the proportion of irregular/peculiar/merger galaxies at $I < 22$ mag determined directly from the raw *HST* images is a factor of 2–3 higher than is determined from *B*-band

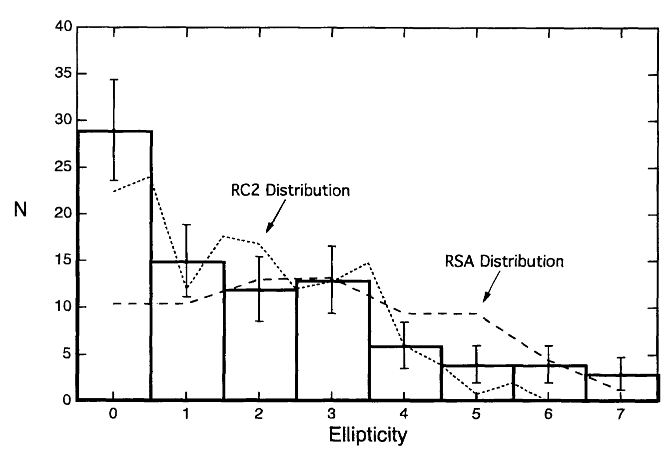


FIG. 8.—Histograms showing the observed distribution of axial ratio among MDS ellipticals. The distributions from the Second Reference Catalog of Bright Galaxies and the Revised Shapley-Ames Catalog are also shown.

[6] For example, bandshifting effects result in the MDS galaxies having very inhomogeneous rest-frame color selection criteria.

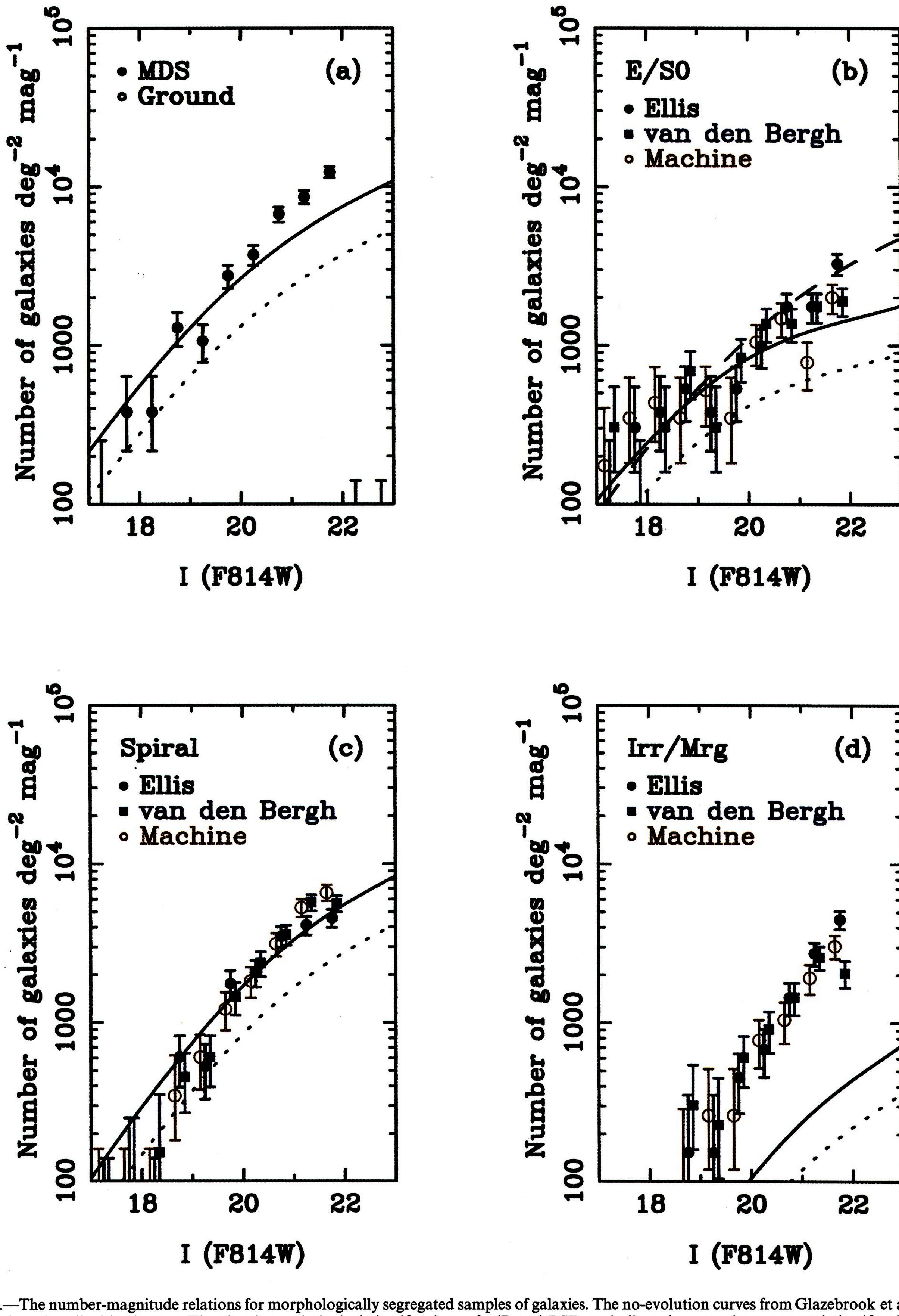


FIG. 7.—The number-magnitude relations for morphologically segregated samples of galaxies. The no-evolution curves from Glazebrook et al. (1995a) are superposed, as described in the text. The visual morphological classifications of vdB and RSE are indicated, as are the automated classifications obtained from position on the *A-C* plane.

magnitude-limited surveys of local galaxies. It is emphasized that larger overdensities of *HST* irregulars/peculiars (such as the factor of $\sim 10$ shown in Fig. 8) are relative to model-dependent extrapolations (to high redshift and faint magnitudes) of the local fraction of irregular/peculiar systems, but that such extrapolations are required in order to account for cosmological effects (e.g., rest-frame color bias) that are not present in local surveys.

Without measured redshifts, knowledge of internal dynamics, or other physical information (such as measures of star formation rates), it is difficult to distinguish between various possibilities for the nature of peculiar galaxies seen on the MDS images. (Possibilities include luminous irregulars, the products of mergers, or a completely new class of objects.) However, the morphological evidence does allow us to constrain the possibilities to some degree, since a lower limit to the fraction of objects with obvious tidal distortions (such as tails) can be estimated. Among the images for which DDO classifications are listed in Table 1, 53 (10.2% $\pm$ 1.4%) exhibit some evidence for tidal distortions (t), and 16 (3.2% $\pm$ 0.8%) possibly show tidal distortions (t: and t?). For comparison, inspection of 935 images of Shapley-Ames galaxies north of $\delta = -27°$ (van den Bergh 1960c) shows that 60 (6.4% $\pm$ 0.8%) nearby galaxies exhibit tidal distortions, while 21 (2.2% $\pm$ 0.5%) show possible (t: and t?) tidal effects. Combining objects classified as t, t: and t? yields 8.7% $\pm$ 1.0% distortions among nearby galaxies, compared to 13.4% $\pm$ 1.6% for the distant *HST* sample is at least 50% larger than it is among nearby galaxies, at the 2 $\sigma$ level.[7] It is emphasized that the true fraction of tidally distorted objects on MDS images may be substantially larger than this lower limit, since clearly defined tidal features are more difficult to detect in the small images of the distant galaxies observed by *HST*. Relatively few "chain galaxies" are seen among the sample of peculiar objects, suggesting that these systems do not form a large component of the peculiar galaxy population at $I < 22$ mag.

Among the 1246 bright galaxies in the revised Shapley-Ames Catalog (Sandage & Tammann 1981), there are seven members of compact groups (Hickson 1995). These objects are NGC 1199 (22a), NGC 3091 (42a), NGC 3190 (44a), NGC 3193 (44b), NGC 3185 (44c), NGC 5353/54 (68a/b), and NGC 5350 (68c). Among the 507 images listed in Table 1, there are at least three, uim0-29/30 and uim0-34, that are located in Hickson-like compact groups. The fraction of galaxies in compact clusters appears to be identical in the Shapley-Ames Catalog (7/1246 = 0.6%) and in the *HST* sample (3/507 = 0.6%). It is of some interest to note that the two Hickson-like compact clusters in the *HST* sample are located less than 1′ apart in the sky.

[7] We stress that the fraction of tidally distorted objects in the Shapely-Ames sample and in the *HST* sample were determined by the *same observer* adopting the same classification criteria for both samples (although the classifications were made 35 years apart). Having the same observer calibrate both local and *HST* samples is obviously important given the systematics described in this paper.

## 5. SUMMARY AND CONCLUSIONS

Classification of the small images of very distant galaxies is both difficult and uncertain. This is so because such classifications require considerable extrapolation from the bright local Hubble-type classification standards. However, the good agreement between the visual and automated classifications for $I < 21$ mag presented in this paper suggests that robust results can be obtained for relatively bright objects within fairly broad morphological bins ($\sim$3–4 Revised Hubble *T*-types). The most subjective factor in the morphological classifications appears to be the determination of the precise nature of "peculiarity" in galaxy images, and for $I > 21$ mag this uncertainty can impact seriously the reliability of morphological classifications. For these fainter galaxies, automated classifications based on central concentration and asymmetry appear to be as reliable as visual classifications, and they have the benefit of objectivity, so that reliable comparisons of the results from different investigations can be made.

All samples of morphological classifications in this paper confirm the good agreement between the observed galaxy counts and no-evolution predictions for the elliptical and spiral populations, as well as the overdensity of peculiar/irregular galaxies relative to the predictions of no-evolution models, reported in Glazebrook et al. (1995a). The faint-end ($I > 21.0$ mag) slope of the number count relation for peculiar objects is defined poorly due to the uncertainties in the visual classifications of irregular/peculiar/merging systems, and it may be somewhat shallower than initially reported. The physical nature of the "*HST* Peculiars" cannot be ascertained from morphological data alone, but some support for the hypothesis that these objects are tidally distorted is given by the fact that the fraction of objects exhibiting tidal tails appears to be at least 50% larger for distant galaxies than it is among nearby ones. This effect appears to be particularly significant because tidal disturbances and tidal tails are more difficult to detect in distant galaxies than they are in nearby objects, unless strong star formation in the tidal debris counteracts the effects of $(1 + z)^4$ surface brightness dimming.

We are indebted to Steve Maddox for useful suggestions, and to Michael Pierce for providing us with a number of CCD images of local reference galaxies in advance of publication. We also thank Ofer Lahav, Avi Naim, Howard Yee, and Frank Valdes for many interesting discussions regarding galaxy classification. Zsolt Frei and James Gunn deserve many thanks (and not only from us) for their public-spirited decision to make their sample of CCD images freely available. We also thank Dennis Crabtree for help with displaying the *HST* images, and Paul Hickson for information on compact groups. Thanks are also due to David Duncan and Janet Currie for help in the preparation of early versions of the manuscript.

## REFERENCES

Abraham, R. G., Valdes, F., Yee, H. K. C., & van den Bergh, S. 1994, ApJ, 432, 75 (Paper I)
Abraham, R. G., et al. 1997, in preparation
Broadhurst, T., Ellis, R., & Shanks, T. 1988, MNRAS, 235, 827
Butcher, H., & Oemler, A. 1978, ApJ, 219, 18
Colless, M., Ellis, R. S., Taylor, K., & Hook, R. N. 1990, MNRAS, 244, 408
Cowie, L. L., Gardner, J. P., Hu, E. M., Songaila, A., Hodapp, K. W., & Wanscoat, R. J. 1994, ApJS, 94, 461
Cowie, L. L., Hu, E. M., & Songaila, A. J. 1995, AJ, 110, 1576
Crampton, D., Le Févre, O., Lilly, S. J., & Hammer, F. 1995, preprint
de Vaucouleurs, G., de Vaucouleurs, A., & Corwin, H. G. 1976, Second Reference Catalog of Bright Galaxies (Austin: Univ. Texas Press)
de Vaucouleurs, G., de Vaucouleurs, A., Corwin, H. G., Buta, R. J., Paturel, G., & Fouqué, P. 1991, Third Reference Catalog of Bright Galaxies (New York: Springer)
Doi, M., Fukugita, M., & Okamura, S. 1993, MNRAS, 164, 832

Driver, S. P., Windhorst, R. A., & Griffiths, R. E. 1995, ApJ, 453, 48
Efstathiou, G., Ellis, R. S., & Peterson, B. A. 1988, MNRAS, 232, 431
Ellis, R. S. 1990, in Kron R. G., ed., ASP Conf. Ser. Vol. 10, Evolution of the Universe of Galaxies, ed. R. G. Kron (San Francisco: ASP), 248
Frei, Z., Guthakurta, P., & Gunn, J. E. 1996, AJ, 111, 174
Glazebrook, K., Ellis, R. S., Colless, M. M., Broadhurst, T. J., Allington-Smith, J. R., & Tanvir, N. R. 1995b, MNRAS, 273, 157
Glazebrook, K., Ellis, R., Santiago, B., & Griffiths, R. 1995a, MNRAS, 275, L19
Griffiths, R. E., et al. 1994, ApJ, 435, 19
Hickson, P. 1995, private communication
Hubble, E. 1936, The Realm of the Nebulae (New Haven: Yale Univ. Press)
Koo, D. C., & Kron, R. 1992, ARA&A, 30, 613
Lilly, S. J. 1993, ApJ, 411, 401
Loveday, J., Peterson, B. A., Efstathiou, G., & Maddox, S. J. 1992, ApJ, 390, 338
Marzke, R. O., Geller, M. J., Huchra, J. P., & Corwin, H. G. 1994, AJ, 108, 437
Morgan, W. W. 1958, PASP, 70, 364
Naim, A., et al. 1995, MNRAS, 274, 1107
Sandage, A., & Tammann, G. A. 1981, A Revised Shapley-Ames Catalog of Bright Galaxies (Washington, DC: Carnegie Inst.)
Schade, D., Lilly, S. J., Crampton, D., Hammer, F., Le Févre, O., & Tresse, L. 1995, ApJ, 451, L1
Shapley, H. 1927, Harvard Obs. Bulletin, 846
Surma, P., et al. 1996, in preparation
Tresse, L., Hammer, F., Le Févre, O., & Proust, D. 1993, A&A, 277, 53
Tufte, E. R. 1993, The Visual Display of Quantitative Information (Connecticut: Graphics Press)
Tyson, J. A. 1988, AJ, 96, 1
van den Bergh, S. 1960a, ApJ, 131, 215
———. 1960b, ApJ, 131, 558
———. 1960c, Publ. David Dunlap Obs., 2, 159
van den Bergh, S., Pierce, M. J., & Tully, R. B. 1990, ApJ, 359, 4